AD-A086 729 NAVAL RESEARCH LAB WASHINGTON DC F/G 20/9
THE NONLINEAR DYNAMICS OF MHD UNSTABLE PLASMAS.(U)
MAY 80 W M MANHEIMER
UNCLASSIFIED NRL-MR-4175 SBIE-AD-E000 453 NL

END
DATE FILMED
8-80
DTIC

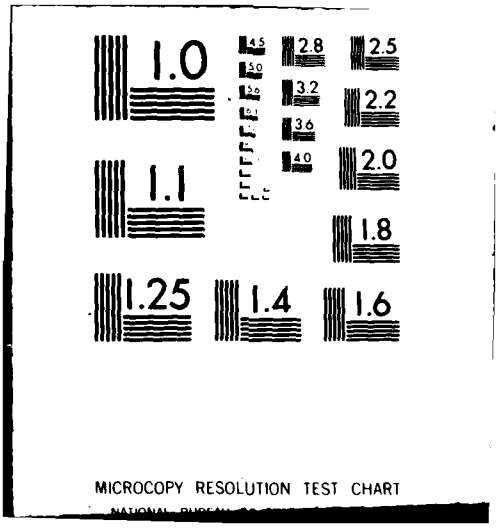
1.0
1.1
1.25
1.4
1.6
1.8
2.0
2.2
2.5
2.8
3.2
3.6
4.0
4.5
5.0
MICROCOPY RESOLUTION TEST CHART

(14) NRL-MR-4175 (9) Memorandum rept.,

SECURITY CLASSIFICATION OF THIS PAGE (When Data Entered)

REPORT DOCUMENTATION PAGE

READ INSTRUCTIONS BEFORE COMPLETING FORM

1. REPORT NUMBER: NRL Memorandum Report 4175	2. GOVT ACCESSION NO.: AD-A086 729
3. RECIPIENT'S CATALOG NUMBER: 1	
4. TITLE (and Subtitle): (6) THE NONLINEAR DYNAMICS OF MHD UNSTABLE PLASMAS	5. TYPE OF REPORT & PERIOD COVERED: Interim report on a continuing NRL problem.
	6. PERFORMING ORG. REPORT NUMBER
7. AUTHOR(s): (10) Wallace M. Manheimer	8. CONTRACT OR GRANT NUMBER(s)
9. PERFORMING ORGANIZATION NAME AND ADDRESS: Naval Research Laboratory, Washington, D.C. 20375	10. PROGRAM ELEMENT, PROJECT, TASK AREA & WORK UNIT NUMBERS: NRL Problem 67-0896-0-0
11. CONTROLLING OFFICE NAME AND ADDRESS: U.S. Department of Energy, Washington, D.C. 20545	12. REPORT DATE: May 12, 1980 (11) 12 May 80
	13. NUMBER OF PAGES: 68 (12) 69
14. MONITORING AGENCY NAME & ADDRESS(if different from Controlling Office): (18) SRIE (19) DD-E000 453	15. SECURITY CLASS. (of this report): UNCLASSIFIED
	15a. DECLASSIFICATION/DOWNGRADING SCHEDULE

16. DISTRIBUTION STATEMENT (of this Report)

Approved for public release; distribution unlimited.

17. DISTRIBUTION STATEMENT (of the abstract entered in Block 20, if different from Report)

18. SUPPLEMENTARY NOTES

19. KEY WORDS (Continue on reverse side if necessary and identify by block number)

MHD instabilities
Nonlinear theory

20. ABSTRACT (Continue on reverse side if necessary and identify by block number)

This is a continuation of NRL Memorandum Report 4000 and it discusses the nonlinear theory of MHD instabilities.

DD FORM 1 JAN 73 1473 EDITION OF 1 NOV 65 IS OBSOLETE
S/N 0102-014-6601

SECURITY CLASSIFICATION OF THIS PAGE (When Data Entered)

25120

CONTENTS

THE NONLINEAR DYNAMICS OF MHD UNSTABLE PLASMAS

X. Quasi-Linear Theory of MHD Instabilities

This chapter begins the second part of this book, that concerning the nonlinear theory of MHD instabilities. Before commencing it is necessary to point out that the nonlinear theory of MHD instabilities is not nearly as well developed as the linear theory and much of what will be discussed here is necessarially more speculative than the material discussed in the preceeding chapters, which treated the linear theory.

We begin by examing the quasi-linear theory of MHD instabilities in which the perturbed velocities are non-singular. This applies potentially to m = 1 kink tearing modes and double tearing modes (Chapters VIII E and F) as well as to ideal MHD modes. In this and the next chapter we change the notation slightly from that in the previous chapters. Now any quantity (say A) will be denoted by $\langle A \rangle + \tilde{A}$ where $\langle A \rangle$ is the ensemble average and $\tilde{A}$ is the perturbation about the ensemble average. Ensemble averaging will be denoted by triangular brackets

For instance, if we restrict ourself to cylindrical geometry, A is a function of radius only, and

$$\tilde{A} = \sum_{m=k\neq 0} A(r,m,k) \exp i(kz+m\theta) + c.c. \qquad \text{(X 1)}$$

the $\neq 0$ under the summation indicating m and k are not both = 0. Since any physical quantity must be real, the complex conjugate is added on in Eq. (X 1). The process of taking the ensemble average can then be defined as an average over θ from zero to 2π and an average over z from 0 to L, where L is either a periodicity length if such a length exists or else is some very large length. Clearly $\langle \tilde{A} \rangle = 0$, but

$$\langle \tilde{A}\,\tilde{B} \rangle = \sum_{k,m\neq 0} A(r,m,k)\, B^{*}(r,m,k) + c.c. \qquad \text{(X 2)}$$

Manuscript submitted March 7, 1980.

Expressing the fluid quantities in this way, the four fluid equations for ρ, $\underline{v}$, $\underline{B}$ and p become

$$\frac{\partial}{\partial t}\left(\langle\rho\rangle+\tilde{\rho}\right)+\ \underline{\nabla}\cdot\left(\langle\rho\rangle+\tilde{\rho}\right)\left(\langle\underline{v}\rangle+\tilde{\underline{v}}\right)=0 \qquad \text{(a)} \qquad \text{(X 3)}$$

$$\left(\langle\rho\rangle+\tilde{\rho}\right)\frac{\partial}{\partial t}\left(\langle\underline{v}\rangle+\tilde{\underline{v}}\right)+\left(\langle\rho\rangle+\tilde{\rho}\right)\left(\langle\underline{v}\rangle+\tilde{\underline{v}}\right)\cdot\underline{\nabla}\left(\langle\underline{v}\rangle+\tilde{\underline{v}}\right)=-\nabla\tilde{p}$$
$$+\frac{1}{4\pi}\left\{\underline{\nabla}\times\left(\langle\underline{B}\rangle+\tilde{\underline{B}}\right)\right\}\times\left(\langle\underline{B}\rangle+\tilde{\underline{B}}\right) \qquad \text{(b)}$$

$$\frac{\partial}{\partial t}\left(\langle\underline{B}\rangle+\tilde{\underline{B}}\right)=\ \underline{\nabla}\times\left(\langle\underline{v}\rangle+\tilde{\underline{v}}\right)\left(\langle\underline{B}\rangle+\tilde{\underline{B}}\right) \qquad \text{(c)}$$

$$\frac{\partial}{\partial t}\left(\langle p\rangle+\tilde{p}\right)+\left(\langle\underline{v}\rangle+\tilde{\underline{v}}\right)\cdot\underline{\nabla}\left(\langle p\rangle+\tilde{p}\right)+\ \frac{5}{3}\left(\langle p\rangle+\tilde{p}\right)\underline{\nabla}\cdot\left(\langle\underline{v}\rangle+\tilde{\underline{v}}\right)=0 \qquad \text{(d)}$$

where we have assumed $\gamma = 5/3$ to avoid confusion between the adiabadic γ and the growth rate.

The first step is to take the ensemble average of (Eqs. X 3). The result is

$$\frac{\partial\langle\rho\rangle}{\partial t}+\ \underline{\nabla}\cdot\rho\underline{v}=-\underline{\nabla}\langle\tilde{\rho}\,\tilde{\underline{v}}\rangle \qquad \text{(a)} \qquad \text{(X 4)}$$

$$\langle\rho\rangle\frac{\partial\langle\underline{v}\rangle}{\partial t}+\langle\rho\rangle\langle\underline{v}\rangle\cdot\underline{\nabla}\langle\underline{v}\rangle+\underline{\nabla}\langle p\rangle-\frac{1}{4\pi}\left(\underline{\nabla}\times\langle\underline{B}\rangle\right)\times\langle\underline{B}\rangle=-\left\langle\tilde{\rho}\frac{\partial}{\partial t}\tilde{\underline{v}}\right\rangle$$
$$-\langle\tilde{\rho}\,\tilde{\underline{v}}\rangle\cdot\underline{\nabla}\langle\underline{v}\rangle-\langle\tilde{\rho}\langle\underline{v}\rangle\cdot\underline{\nabla}\,\tilde{\underline{v}}\rangle-\langle\rho\rangle\langle\tilde{\underline{v}}\cdot\underline{\nabla}\,\tilde{\underline{v}}\rangle-\langle\tilde{\rho}\,\tilde{\underline{v}}\cdot\underline{\nabla}\,\tilde{\underline{v}}\rangle$$
$$+\frac{1}{4\pi}\left\langle\left(\underline{\nabla}\times\tilde{\underline{B}}\right)\times\tilde{\underline{B}}\right\rangle \qquad \text{(b)}$$

$$\frac{\partial\langle\underline{B}\rangle}{\partial t}-\underline{\nabla}\times\langle\underline{v}\rangle\times\langle\underline{B}\rangle=\underline{\nabla}\times\langle\tilde{\underline{v}}\times\tilde{\underline{B}}\rangle \qquad \text{(c)}$$

$$\frac{\partial\langle p\rangle}{\partial t}+\langle\underline{v}\rangle\cdot\underline{\nabla}\langle p\rangle+\frac{5}{3}\langle p\rangle\underline{\nabla}\cdot\langle\underline{v}\rangle=-\langle\tilde{\underline{v}}\cdot\underline{\nabla}\tilde{p}\rangle-\frac{5}{3}\langle\tilde{p}\,\nabla\cdot\tilde{\underline{v}}\rangle \qquad \text{(d)}$$

Then subtracting Eqs. (X 4) from Eqs. (X 3) gives the equations

$$\frac{\partial \tilde{\rho}}{\partial t} + \nabla \cdot \left(\tilde{\rho} \langle \underline{v} \rangle + \langle \rho \rangle \tilde{\underline{v}} \right) = - \left(\nabla \cdot \tilde{\rho} \tilde{\underline{v}} - \nabla \cdot \langle \tilde{\rho} \tilde{\underline{v}} \rangle \right) \qquad (a)$$

$$\langle \rho \rangle \frac{\partial \tilde{\underline{v}}}{\partial t} + \tilde{\rho} \frac{\partial \langle \underline{v} \rangle}{\partial t} + \tilde{\rho} \langle \underline{v} \rangle \cdot \nabla \langle \underline{v} \rangle + \rho \tilde{\underline{v}} \cdot \nabla \langle \underline{v} \rangle + \langle \rho \rangle \langle \underline{v} \rangle \cdot \nabla \tilde{\underline{v}} + \nabla \tilde{p}$$

$$- \frac{1}{4\pi} \left\{ \left(\nabla \times \tilde{\underline{B}} \right) \times \langle \underline{B} \rangle + \left(\nabla \times \langle \underline{B} \rangle \right) \times \tilde{\underline{B}} \right\} = - \tilde{\rho} \frac{\partial \tilde{\underline{v}}}{\partial t} + \left\langle \tilde{\rho} \frac{\partial \tilde{\underline{v}}}{\partial t} \right\rangle$$

$$- \tilde{\rho} \tilde{\underline{v}} \cdot \nabla \langle \underline{v} \rangle + \langle \tilde{\rho} \tilde{\underline{v}} \rangle \cdot \nabla \langle \underline{v} \rangle - \tilde{\rho} \langle \underline{v} \rangle \cdot \nabla \tilde{\underline{v}} + \left\langle \tilde{\rho} \langle \underline{v} \rangle \cdot \nabla \tilde{\underline{v}} \right\rangle$$

$$- \langle \rho \rangle \tilde{\underline{v}} \cdot \nabla \tilde{\underline{v}} + \langle \rho \rangle \langle \tilde{\underline{v}} \cdot \nabla \tilde{\underline{v}} \rangle - \tilde{\rho} \tilde{\underline{v}} \cdot \nabla \tilde{\underline{v}} + \langle \tilde{\rho} \tilde{\underline{v}} \cdot \nabla \tilde{\underline{v}} \rangle$$

$$+ \frac{1}{4\pi} \left(\nabla \times \tilde{\underline{B}} \right) \times \tilde{\underline{B}} - \frac{1}{4\pi} \left\langle \left(\nabla \times \tilde{\underline{B}} \right) \times \tilde{\underline{B}} \right\rangle \qquad (b)$$

(X 5)

$$\frac{\partial \tilde{\underline{B}}}{\partial t} - \nabla \times \tilde{\underline{v}} \times \langle \underline{B} \rangle - \nabla \times \langle \underline{v} \rangle \times \tilde{\underline{B}} = \nabla \times \tilde{\underline{v}} \times \tilde{\underline{B}} - \nabla \times \langle \tilde{\underline{v}} \times \tilde{\underline{B}} \rangle \qquad (c)$$

$$\frac{\partial \tilde{p}}{\partial t} + \tilde{\underline{v}} \cdot \nabla \langle p \rangle + \langle \underline{v} \rangle \cdot \nabla \tilde{p} + \frac{5}{3} \tilde{p} \nabla \cdot \langle \underline{v} \rangle + \frac{5}{3} \langle p \rangle \nabla \cdot \tilde{\underline{v}} =$$

$$- \tilde{\underline{v}} \cdot \nabla \tilde{p} + \langle \tilde{\underline{v}} \cdot \nabla \tilde{p} \rangle - \frac{5}{3} \tilde{p} \nabla \cdot \tilde{\underline{v}} + \frac{5}{3} \langle \tilde{p} \nabla \cdot \tilde{\underline{v}} \rangle \qquad (d)$$

Equations (X 4 a-d) and Equations (X 5 a-d) are now a complete set of non-linear equations for $\langle\rho\rangle, \tilde{\rho}, \langle\underline{V}\rangle, \tilde{\underline{V}}, \langle\underline{B}\rangle, \tilde{\underline{B}}, \langle p\rangle$ and $\tilde{p}$, and so far no approximations have been made.

The quasi-linear approximation to these equations consists of neglecting the $\langle \tilde{\rho}\tilde{\underline{V}}\cdot\nabla\tilde{\underline{V}} \rangle$ term (that is the term cubic in fluctuating quantities) from the right hand side of Eq. (X 4b) and in neglecting the entire right hand side of Eqs. (X 4 a-d). We will briefly discuss these approximations now. The fluctuating quantities are assumed to be small so that a term like $\langle\tilde{\rho}\tilde{\underline{V}}\cdot\nabla\tilde{\underline{V}}\rangle$ is expected to be much smaller than a term like $\rho\langle\tilde{\underline{V}}\cdot\nabla\tilde{\underline{V}}\rangle$ since $\tilde{\rho}<<\rho$. This is the basic justification for neglecting the cubic nonlinear terms on the right hand side of Eq. (X 4b).

Notice that all terms on the right hand side of Eqs. (X 5 a-d) are various quantities minus their ensemble averages. This ensures that for our cylindrical case of azimuthal and axial averaging, there is no quantity on the right hand side of Eqs. (X 5a-d) which is a function of only r. That is every driving term on the right hand side has oscilliatory structure in θ and/or z. For instance if there are two fluctuations at (k_1,m_1) and (k_2,m_2), the quadratic terms on the right hand side will drive additional fluctuations at $(2k_1, 2m_1)$, $(2k_2, 2m_2)$ and $(k_1 \pm k_2, m_1 \pm m_2)$. However no fluctuation will be driven at $k = m = 0$ since the ensemble (ie azimuthal and axial) average average of the right hand side is subtracted out. These terms then describe the coupling of fluctuations at different wave lengths directly with each other.

Thus the quasi-linear approximation neglects coupling of the fluctuations among themselves, but includes the coupling (correct to second order) of the fluctuating to ensemble average quantities. Therefore the basic idea behind

the quasi-linear approximation is that coupling of the waves to the background is somehow more important than the coupling of the waves to each other.

With the right hand side of Eqs. (X 5 a-d) set equal to zero, the equations for the tildad quantities are very similar to the linearized fluid equations of earlier chapters, but with two important complications. First of all the background velocity is not equal to zero in Eqs. (X 5 a-d) and secondly, the background quantities are functions of time as well as radius. To proceed, we now restrict ourselves to the lowest order tokamak ordering and to systems not far above stability threshold. As we will now show, these complications can then be eliminated. In lowest order tokamak ordering, recall $B_z >> B_\theta$, $R >> a$ and the mode structure is two dimensional in the $r\theta$ plane (that is $\tilde{V}_z = \tilde{B}_z = 0$). Also $\nabla \cdot \tilde{V} = 0$, that is, the perturbation is incompressible. The equation for B_z, from Eq. (X 4c) then becomes

$$\frac{\partial B_z}{\partial t} = - \frac{1}{r} \frac{\partial}{\partial r} r V_r B_z \qquad \text{(X 6)}$$

Since B_z is very large, it cannot change very much without drastically altering the systems energy density. However for B_z to remain unchanged, it must be that

$$V_r \approx 0 \qquad \text{(X 7)}$$

Thus to lowest order in tokamak ordering, the ensemble average radial velocity vanishes. Now let us consider the azimuthal and axial component of velocity. Making use of the fact that the fluctuating flow and magnetic field are incompressible in two dimensions, it is a straight forward matter to show that the θ and z components of the terms on the right hand side of Eq. (X 4b) are proportional to $V_\theta \frac{\partial V_z}{\partial r}$ and $\frac{\partial V_\theta}{\partial r}$.

Thus there is no term which acts as a source term for an acceleration in θ and z (one can also show that this is true in cylindrical geometry without an expansion in tokamak ordering). Therefore, if V_θ and V_z are initially zero, they will be zero at all subsequent time. Hence, to lowest order in tokamak ordering, there is no induced fluid velocity, or

$$\underline{V} = 0 \tag{X 8}$$

(In general in cylindrical geometry $V_z = V_\theta = 0$, but $V_r \neq 0$.)

In this case the equation for the perturbed quantities (Eqs. (X 5 a-d) with the right hand side = 0) are different from the linearized equations in previous chapters only in that the background quantities are functions of time. Therefore the perturbed quantities cannot be assumed to have a time dependence like exp γt. However if the time scale for the change of equilibrium quantities, τ_{eq} satisfies the condition

$$\gamma \tau_{eq} << 1 \tag{X 9}$$

where γ is the linear growth rate (assuming the ensemble average quantities are time invariant), then one can solve Eqs. (X 5 a-d) by making a WKB approximation. That is, fluctuating quantities are proportional to $\exp \int \gamma(t)dt$. The zero order WKB approximation to Eqs. (X 5 a-d) then give the conventional result

$$\gamma \tilde{\rho} + \underline{V} \cdot \nabla \langle \rho \rangle (t) = 0 \qquad (a)$$

$$\gamma \langle \rho(t) \rangle \tilde{V} = -\nabla \tilde{p} + \frac{1}{4\pi} \left\{ (\nabla \times \tilde{\underline{B}}) \times \langle \underline{B}(t) \rangle + (\nabla \times \langle B(t) \rangle \times \tilde{B}) \right\} \qquad (b)$$

$$\gamma \tilde{B} = \nabla \times \tilde{V} \times \langle B(t) \rangle \qquad (c) \tag{X 10}$$

$$\nabla \cdot \tilde{V} = 0 \qquad (d)$$

where we have assume the flow is incompressible in Eq. (X 10d). These are just the conventional equations for perturbed quantities which we have studied in previous sections. Using them to express $\tilde{\rho}$, $\tilde{B}$ and $\tilde{p}$ in terms of $\tilde{V}$, it is a simple matter to show that the equations for ρ,p, and B_θ are

$$\frac{\partial \langle \rho \rangle}{\partial t} = \frac{1}{r}\frac{\partial}{\partial r} r \sum_{mk} \gamma \left\langle \tilde{\xi}_r^2(r,m,k) \right\rangle \frac{\partial \langle \rho \rangle}{\partial r} \qquad \text{(a)}$$

$$\frac{\partial \langle p \rangle}{\partial t} = \frac{1}{r}\frac{\partial}{\partial r} r \sum_{mk} \gamma \left\langle \xi_r^2(r,m,k) \right\rangle \frac{\partial p}{\partial r} \qquad \text{(b)} \qquad \text{(X 11)}$$

$$\frac{\partial \langle B_\theta \rangle}{\partial t} = \frac{\partial}{\partial r}\frac{1}{r}\frac{\partial}{\partial r} \sum_{mk} \frac{\gamma}{m} \left\{ \left\langle \xi_r^2(r,m,k) \right\rangle r^2 \left(\frac{m\langle B_\theta \rangle}{r} + k\langle B_z \rangle \right) \right\} \qquad \text{(c)}$$

where $\tilde{\xi}_r$ is the radial displacement, $\tilde{\xi}_r = \tilde{V}_r/\gamma$ and where as usual the perturbation is assumed to be a summation of individual fluctuations proportional to exp (im θ + ikz). It only remains to check a postiori that Eq. (X 9) is satisfied. If r_n is the radial scale length for say the density variation, Eq. (X 9) reduces to

$$\xi_r \ll L_n \qquad \text{(X 12)}$$

Thus Eq. (X 9) is satisfied as long as the radial displacement is small compared to the radial scale length.

Equations (X 11 a-c) then describe the evolution of the background density, pressure and poloidal field in response to the instability. These equations in themselves do not guarantee pressure balance. However pressure balance can easily be maintained through very small changes in B_z. Thus we expect that V_r will not exactly vanish, but rather that there will be a very small V_r which will modify very slightly, B_z (according to Eq. (X 6)) so as to maintain pressure balance at all times.

To summarize, the quasi-linear approximation is that the instability grows at its temporarilly local linear growth rate and that the background plasma slowly reacts to the presence of this instability, modifying its growth rate. To our knowledge, no general conditions under which quasi-linear theory is valid have been given. Clearly it is not valid in a situation like fluid turbulence where the main interaction is the modes with each other rather than the modes with the background. The quasi-linear theory is most likely to be valid in a situation where a plasma is initially weakly unstable and where the subsequent growth of instability causes it to evolve, according to Eqs. (X 11 a-c) to a stable state. It is least likely to be valid in a condition of steady state or fully developed turbulence.

An interesting related observation is that the quasi-linear theory of velocity space instabilities has been widely studied for infinite homogeneous plasmas. There, comparisons between quasi-linear theory and particle simulation has frequently shown that quasi-linear theory does provide a reasonably accurate approximation of the description of the evolution of an initially unstable plasma to a final stable state.

There is one aspect of Eqs. (X 11 a and c) which might at first appear paradoxical. That is the ensemble average magnetic field is no longer frozen into the ensemble average flow. This can most easily be seen in slab geometry. If the perturbation is two dimensional and incompressible in the xy plane, a simple calculation shows that the slab geometry analogs to Eqs. (X 11 a and c) are

$$\frac{\partial \langle \rho \rangle}{\partial t} = \frac{\partial}{\partial x} \gamma \langle \tilde{\xi}_x^2 \rangle \frac{\partial \langle \rho \rangle}{\partial x} \qquad (a)$$

$$\frac{\partial \langle B_y \rangle}{\partial t} = \gamma \frac{\partial^2}{\partial x^2} \langle \tilde{\xi}_x^2 \rangle \langle B_y \rangle \qquad (b) \qquad (X\ 13)$$

Since $V_x = 0$, frozen in field means ρ/B_y is constant which clearly is not the case if ρ and B_y obey Eqs. (X 13).

The resolution of this apparent paradox comes from the fact that the MHD constraint does not require the average field to be frozen into the average density; rather it requires that the exact field be frozen into the exact flow. The two requirements are not the same as we will now show. To show this imagine a fluid with initial density $\rho_o(x)$ and field $B_o(x)\ \underline{i}_y$. Then give each element of the fluid a displacement $\xi \sin ky\ \underline{i}_x$ where ξ is constant. Let us now calculate the new density and magnetic field. To do consider 3 neighboring points initially at (x,y), (x + dx, y) and (x, y + dy). After displacement, these points go to $(x + \xi \sin ky, y)$, $(x + dx + \xi \sin ky, y)$, and $(x + \xi \sin ky + kdy \cos ky, y + dy)$. The two difference vectors before and after the displacement are $dx\underline{i}_x$ and $dy\ \underline{i}y$ before; and $dx\underline{i}_x$ and $\xi\ dy\ k \cos ky\ \underline{i}_x + dy\ \underline{i}y$ after. The original and final area is dxdy, as can be seen by taking cross products of the two sets of difference vectors. This confirms the incompressible character of the displacement. Thus if the initial position of a point (ie (x,y)) is denoted $\underline{r}_o$, and the final position $(x + \xi \sin ky, y)$ is denoted $\underline{r}$, then

$$\rho_o(\underline{r}_o) = \rho(\underline{r}) \qquad \text{(X 14)}$$

Solving for $\underline{r}_o$ in terms of $\underline{r}$, we have

$$\rho(\underline{r}) = \rho_o\left(x - \xi \sin ky\right) \qquad \text{(X 15)}$$

Assuming that the variation of ρ_o is small in a distance ξ, we find that the density averaged over y is given approximately by

$$\langle \rho(x) \rangle = \rho_o(x) + \frac{1}{4}\xi^2 \frac{\partial^2 \rho_o}{\partial x^2} \qquad \text{(X 16)}$$

We will now continue by calculating the field, exploiting the fact that it is frozen into the flow. In the undisplaced fluid, the field is parallel to the first difference vector dy $\underline{i}_y$. This difference vector is displaced to dy (ξ k cos ky $\underline{i}_x$ + $\underline{i}_y$) and this must be parallel to the 'displaced' field. Thus a unit vector parallel to B is

$$\underline{i}_B = \frac{\xi k \cos ky \; \underline{i}x + \underline{i}_y}{(1 + \xi^2 k^2 \cos^2 ky)^{1/2}} \qquad \text{(X 17)}$$

Now calculate the magnitude of $\underline{B}$. The initial flux through the line $\{(x + dx, y) - (x,y)\}$ is $(B_0(x)\underline{i}_y)\cdot(dx\underline{i}_y) = B_0(x_0)dx$. After displacement flux is frozen in, so

$$B(\;)\underline{i}_B \cdot i_y dx = B_0(x_0)dx_0, \quad \text{or}$$

$$B(r) = B_0(x_0)\left((\xi k \cos ky)^2 + 1\right)^{1/2} = B_0(x - \xi \sin ky)\left((\xi k \cos ky)^2 + 1\right)^{1/2} \qquad \text{(X 18)}$$

The y component of B in the displaced fluid is

$$B_y = B(r)\,\underline{i}_B \cdot i_y = B_0(x - \xi \cos ky) \qquad \text{(X 19)}$$

Again, assuming that B_0 varies only slightly in a distance ξ, we find

$$\langle B_y \rangle = B_0(x) + \frac{1}{4}\xi^2 \frac{\partial^2 B_0}{\partial x^2} \qquad \text{(X 20)}$$

As is apparent from Eqs. (X 16 and 20), $\langle\rho\rangle/\langle B_y\rangle \neq n/B$ so the average field is not frozen into the average density. Yet the field was calculated by making explicit use of the fact that the exact field is frozen into the exact density. Therefore ensemble averaging destroys the 'frozen in' nature of magnetic fields in ideal MHD.

In a sense, this is not a surprising result. As we have seen in Chapter VII and VIII, fluid flow with frozen in field can lead to very complicated, small scale magnetic structures which may well be completely washed out with any kind of ensemble averaging. However, this complicated structure was a direct consequence of frozen in fields, so averaging field and density will in all likelyhood destroy this link.

An analogous situation is an incompressible fluid with variable density $\rho(x)$ filling the square $-L < x,y, < L$. Imagine stirring up this fluid for a long time. Even though the flow is imcompressible,low and high density parts are forced near each other in an almost random way. Hence any kind of coarse grain averaging of the fluid will give rise to nearly uniform density, even though this might at first sight appear to be impossible due to the incompressibility condition. Mixing scotch and soda is a more familiar example of this effect. Therefore, in all cases, 'microscopic' constraints can become unglued upon ensemble averaging.

Let us now apply the quasi-linear theory to an internal m = 1 kink tearing mode. The theory is greatly simplified because ξ_r = constant (that is independent of r) within the q = 1 surface, and only the m = n = 1 mode is assumed to exist. As it can easily be shown that for B_z = constant and $\tilde{\xi}_r$ = constant, there is no contribution to $\frac{\partial B_\theta}{\partial t}$ from B_z, the equation for B_θ is

$$\frac{\partial B_\theta}{\partial t} = \gamma \frac{\partial}{\partial r} \frac{1}{r} \frac{\partial}{\partial r} r \langle \xi^2 \rangle B_\theta \qquad \text{(X 21)}$$

which is very much like a diffusion equation. Another way of writing Eq. (X 21) is to take the curl and write it as an equation for the plasma current in the Z direction. The result

$$\frac{\partial}{\partial t} J_z = \gamma \frac{1}{r} \frac{\partial}{\partial r} r \frac{\partial}{\partial r} \langle \xi^2(t) \rangle J_z \qquad \text{(X 22)}$$

which is a diffusion equation for J_z.

We conclude by examing what sort of an interpretation for m = n = 1 sawtooth oscillations can be made by using quasi-linear theory. Imagine that at time t = 0, an Ohmically heated tokamak discharge has $q(r = 0) < 1$; and, as is usually the case, monotonically decreasing profiles of $\rho(r)$, $p(r)$ and $J_z(r)$ (but monotinically increasing profile of $q(r)$) as shown in Fig. (X 1a). This configuration is unstable to the m = n = 1 kink tearing mode. According to quasi-linear theory, this mode will grow at its local growth rate and ρ, p and J_z all obey diffusion equations. Thus current, density and pressure all diffuse outward, and tend to evolve the plasma to a final state where J_z (and thereby q), ρ and p all have no radial gradient within the singular region, as shown in Fig. (X 1b). Now let us postulate that the steep gradient near the singular surface in Fig. (X 1b) rapidly diffuses away, either by classical diffusion, or more likely by exciting some sort of micro-instability. After this, the profile has smoothed out and looks like that shown in Fig. (X 1c), where the interaction between the m = n = 1 instability and whatever smoothes out the profile, will insure that in the final state, $q(r = 0) \geq 1$, so the plasma is stable. However the plasma is heated by Ohmic heating, so that the hotter central region tends to be preferentially heated. This lowers the resistivity, and channels the current into the center thereby lowering $q(r = 0)$ until it is less than unity. Thus the current channeling tends to force the plasma back into an unstable state. This channeling plus the quasi-linear reaction of the plasma are the two basic components of a relaxation oscillation, very much as observed in the central region of tokamaks.

Let us now see how large ξ_x would be for such a relaxation oscillation. From (Eq. (X 11b) the energy confinement time of the central region is given roughly by

$$\tau_E \sim \left[\gamma \left(\frac{\xi_r}{r_s}\right)^2\right]^{-1} \qquad \text{(X 23)}$$

where r_s is the radius of the singular surface. Let us consider for instance TFR where $T_e \simeq 2$Kev, $\beta_\theta \sim \frac{1}{3}$, $r_s \simeq 10$ cm and $F^1 \sim B_\theta / r_s^2$. Then according to Eq. (VIII 44), $\gamma \sim 10^4$. The fast downstroke of the relaxation oscillation occurs in about one millisecond. Even assuming all of the energy is expelled from the central region in this time, Eq. (X 11b) gives $(\xi_r/r_s) \sim \frac{1}{3}$. Since much less than all of the energy is expelled (recall that the diffusion only flattens the pressure profile within the singular surface), r/r_s is really much less than one third, so at least this aspect of quasi-linear theory appears to be valid. In a later section we will discuss numerical simulations of this instability. While many of the gross features can be described by quasi-linear theory, we will see that the actual description can be quite a bit more complicated.

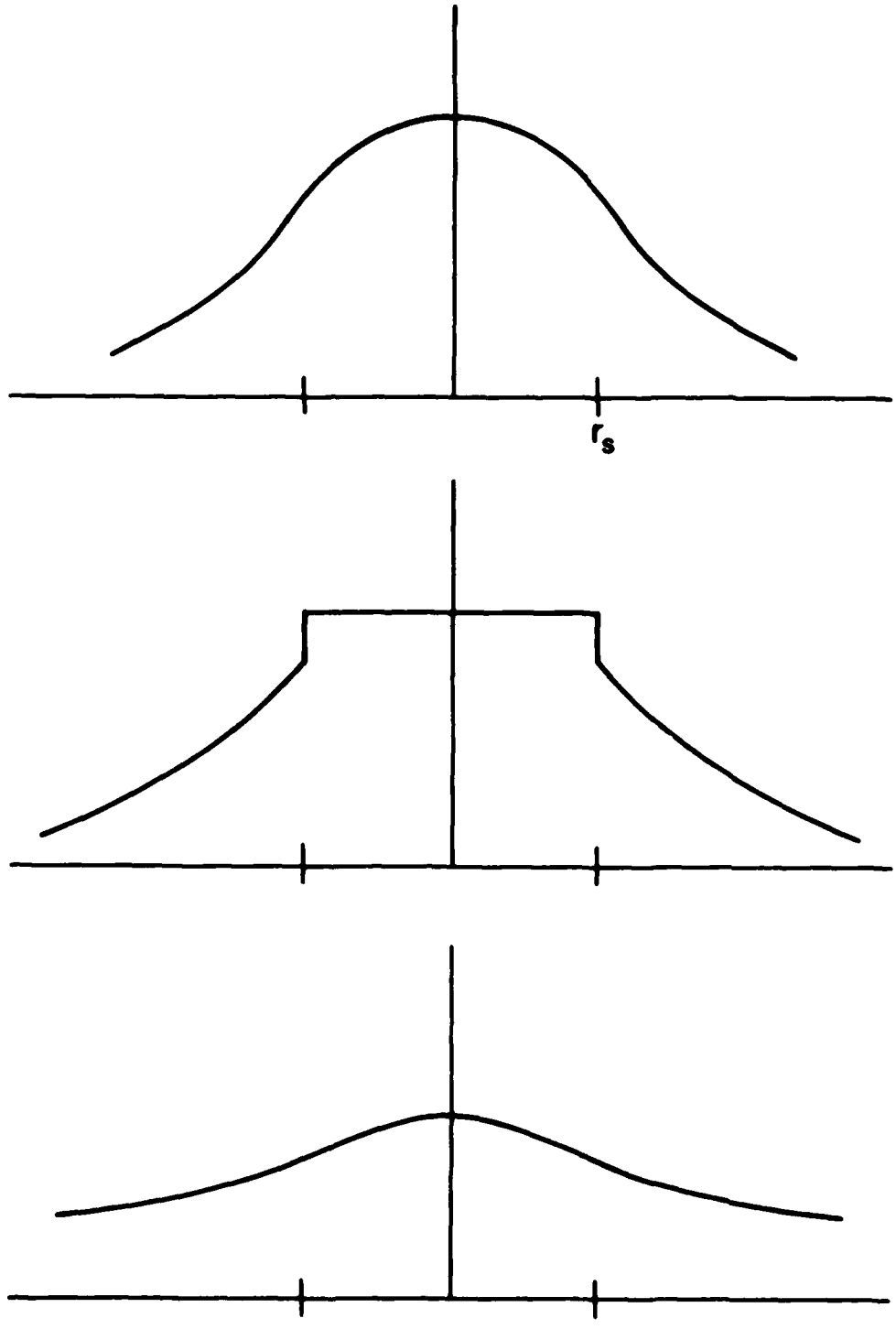

X 1) The quasi-linear evolution of the toroidal current for an m = n = 1 internal kink tearing mode. a) The initial current, b) The current on completion of the MHD instability phase, c) The current after the resulting steep gradients diffuse away.

XI. Quasi-Linear Theory and Rutherford's Nonlinear Theory of Tearing Modes

Since the tearing mode is driven by magnetic energy in the outer region, it is tempting to describe its nonlinear evolution in terms of a quasi-linear theory of only the outer region. In this way, one might be able to follow the growth of the tearing mode coupled to the depletion of free energy which drives it. Then, when all of the free energy is used up, linear growth should stop. Another attractive feature of an outer region quasi-linear theory is that it works the same way no matter what the dissipation mechanism in the inner region is. The problem is that the MHD equation for the outer region is singular, so that one still has to treat the singularity. For instance if $\tilde{B}_x(x,y,t) = \tilde{B}_x(x) \exp i(ky + \gamma t) + c.c.$, then Eq. (X 13b) reduces to

$$\frac{\partial \langle B_y \rangle}{\partial t} = \frac{\partial \gamma}{k^2}\frac{\partial^2}{\partial x^2}\frac{|\tilde{B}_x|^2}{\langle B_y \rangle} = \frac{\gamma}{k}\frac{\partial^2}{\partial x^2} i\tilde{\xi}_x^* \tilde{B}_x + c.c. \qquad \text{(XI 1)}$$

where we have related $\tilde{B}_x$ to the displacement by the ideal MHD relation $\tilde{B}_x = i k \langle B_y \rangle \xi$. Also, as in Chapter X, we have assumed the presence of a large, uniform B_z. Clearly, Eq. (XI 1) is singular at $x = 0$, the position where $\langle B_y \rangle = 0$. For $\langle B_y(x) \rangle$ as shown in Fig. (XI 1a), it is possible to show that in the outer region, the ambient magnetic field loses energy and thereby drives the mode. To do so, make use of the fact that around $x = 0$, because of the nonzero resistivity $\xi(x)$ is actually a well behaved function of x over the entire domain $-\infty < x < \infty$. Therefore, the last form of Eq. XI 1 can be integrated by parts so that

$$\frac{d}{dt}\int_{-\infty}^{\infty} dx \frac{\langle B_y \rangle^2}{2} = \int_{-\infty}^{\infty} \frac{\gamma}{k}\langle B_y \rangle \frac{\partial^2}{\partial x^2} i\tilde{\xi}_x^* \tilde{B}_x + c.c.$$

$$= \int_{-\infty}^{\infty} dx \frac{\gamma}{k} i\tilde{\xi}_x^* \tilde{B}_x \frac{\partial^2}{\partial y^2}\langle B_y \rangle + c.c. = \int \frac{\partial \gamma}{k^2}\frac{|\tilde{B}_x|^2}{\langle B_y \rangle}\frac{\partial^2}{\partial x^2}\langle B_y \rangle \qquad \text{(XI 2)}$$

Since $\langle B_y \rangle = 0$ at $x = 0$, the last integral in Eq. X 2 is not singular. Also B_y and its second derivative everywhere have opposite signs (see fig. (X 1a and b), so it is clear that energy is released from initial magnetic field. This energy goes to drive the tearing mode. Clearly the energy released within the inner region is not accurately calculated; however, this should be unimportant, very little magnetic energy is there in the first place.

We now examine how the quasi-linear evolution of the plasma in the outer region can be carried out. There are two relevant widths in the inner region, first there is the resistive layer size L_c given by Eq. (VII 25c) and secondly there is the island width Δx_{is}. It is clear that Eq. (XI 1) is not valid for $x < L_c$ because all information concerning resistivity was left out. However, it is also true that Eq. (XI 1) cannot be valid for $x < \Delta x_{is}$ either. The reason is that it is a partial differential equation relating the change in $\langle B_y \rangle$ to the spatial structure of $\langle B_y \rangle$ in the immediate neighborhood. However, during reconnection, the magnetic field line is suddenly affected by the other field line it reconnects with; a field line which is generally very far away. Thus the behavior of the ambient field during reconnection cannot be described by a single partial differential equation. This can also be seen in the derivation leading up to Eq. (X 20). From this it is clear that Eq. (XI 1) described the response of the average frozen in field to small displacements of the fluid.

Therefore, Eq. (XI 1) can only be valid both outside the singular layer <u>and</u> outside the island. In the linear regime, where $\tilde{B}$ is infinitesimal, the island width is smaller than the resistive layer width. However since L_c is small, as $\tilde{B}$ grows, soon $\Delta x_{is} > L_c$ so the island width becomes the

relevant inner layer width. Equation (XI 1) then is only valid for $x > \Delta x_{is}$.

We now show how the quasi-linear evolution of a single tearing mode may be carried out. If the variables are renormalized in dimensionless form as

$$\rho = kx \qquad \text{(a)}$$
$$\tau = \int \gamma dt \qquad \text{(b)} \qquad \text{(XI 3)}$$

the equations for $\tilde{B}_x$ and B_y are

$$\frac{\partial^2 \tilde{B}_x}{\partial \rho^2} = \left(1 + \frac{\frac{\partial^2 \langle B_y \rangle}{\partial \rho^2}}{\langle B_y \rangle}\right) \tilde{B}_x \qquad \text{(a)}$$

$$\frac{\partial \tilde{B}_x(\rho=\rho_{is}, \tau)}{\partial \tau} = \tilde{B}(\rho=\rho_{is}, \tau) \qquad \text{(b)} \qquad \text{(XI 4)}$$

$$\frac{\partial}{\partial t}\langle B_y \rangle = \alpha \frac{\partial^2}{\partial \rho^2} \frac{|\tilde{B}_x|^2}{\langle B_y \rangle} = 4 \frac{\tilde{B}_x^2}{\langle B_y \rangle} + \frac{4}{\langle B_y \rangle}\left(\frac{\partial \tilde{B}_x}{\partial \rho}\right)^2$$

$$- \frac{8\tilde{B}_x}{\langle B_y \rangle^2} \frac{\partial \tilde{B}_x}{\partial \rho} \frac{\partial \langle B_y \rangle}{\partial \rho} + \frac{4\tilde{B}_x^2}{\langle B_y \rangle^3}\left(\frac{\partial \langle B_y \rangle}{\partial \rho}\right)^2 \qquad \text{(c)}$$

$$+ \frac{\tilde{B}_x^2}{\langle B_y \rangle^2} \frac{\partial^2 \langle B_y \rangle}{\partial x^2}$$

To get the second form of Eq. (XI 4c), we have expanded the derivatives and used Eq. (XI 4a) to express $\frac{\partial^2 \tilde{B}_x}{\partial x^2}$. Despite the apparent complexity, the second form in Eq. (XI 4c) is much simpler to work with because the diffusion term now has a positive diffusion constant. Also, we have assumed $\tilde{B}_x$ is real. Equation (XI 4a) is the equation for $\tilde{B}_x$ in the outer region (the same as Eq. VII 9) except that now $|\rho| > \rho_{is}$ where $\rho_{is} = 2\left(2\,\tilde{B}_x \Big/ \frac{\partial \langle B_y \rangle}{\partial \rho}\Big|_{\rho = 0}\right)^{1/2}$. (The additional factor of $\sqrt{2}$ between this and Eq. (VII 41) comes from the difference between sin cos and exponential notation). Equation (XI 4b) simply says that the fluctuation at $\rho = \rho_{is}$ grows as the linear growth rate. Equation (XI 4c) is the quasi-linear equation for $\langle B_y \rangle$, which is valid only outside the island, that is $|\rho| > \rho_{is}$.

The question now is how to calculate the island width, which depends upon the slope of $\langle B_y \rangle$ at $x = 0$, that is, inside the singular region. Clearly it is necessary to make some assumption concerning the current and field distribution inside the singular layer. We make the reasonable assumption that $\langle B_y \rangle$ is linear in x within the island. Then Eqs. (4) must be solved numerically in space and time, coupled with a calculation of the island width. The procedure is as follows.

At $\tau = 0$ start with a field profile, which we will specify as $\langle B_y \rangle = B_o \tanh(\rho/L_s)$. Here L_s is the scale length in units of k^{-1}. To advance from τ to $\tau + \Delta\tau$, first solve Eq. (XI 4a) for $\tilde{B}_x$. From $\tilde{B}_x$, calculate

$$\Delta = \frac{1}{\tilde{B}_x(\rho = \rho_{is})}\left\{\frac{\partial \tilde{B}_x}{\partial \rho}\Big|_{\rho_{is}} - \frac{\partial \tilde{B}_x}{\partial \rho}\Big|_{-\rho_{is}}\right\} = \frac{2}{\tilde{B}_x(\rho = \rho_{is})}\frac{\partial \tilde{B}_x}{\partial x}\Big|_{\rho_{is}} \quad \text{(XI 5)}$$

due to the symmetry. Note that now Δ is calculated across the island rather than as a discontinuity at $x = 0$. This means the Δ in Eq. (XI 5) is proportional to the field energy liberated outside the island. If

$\Delta < 0$, the plasma has become stable and the calculation is finished with the $\langle B_y \rangle = \langle B_y(\tau) \rangle$. If $\Delta > 0$ the plasma is still unstable so that $B_y(\rho=\rho_{is},\tau)$ is advanced according to Eq. (XI 4b) and $\langle B_y \rangle$ is advanced according to Eq. (XI c). To calculate the island width first calculate the quantity

$$L_{is}(\rho, \tau+\Delta\tau) = 2\left[2\rho\, \tilde{B}(\rho=\rho_{is}, \tau+\Delta\tau)/\langle B_y(\rho, \tau+\Delta\tau)\rangle\right]^{1/2} \qquad \text{(XI 6)}$$

This is the island width, determined at each ρ, assuming the field inside the island is linear up to that ρ and equal to $\langle B_y(\rho) \rangle$ at ρ. The actual island width is then determined at each time step by solving

$$L_{is}(\rho, \tau+\Delta\tau) = \rho \qquad \text{(XI 7)}$$

and the solution of Eqs. (XI 4a and c) is invoked only outside the island. The field inside the island then is linear in ρ, and Eq. (XI 7) insures that $\langle B_y \rangle$ is continuous at $\rho = L_{is}(\rho, \tau + \Delta\tau)$.

Equations (XI 4a-c) were solved numerically by Dr. Barbara Mellander using this assumption for the field inside the island. The initial and final magnetic fields for four choices of L_s are shown in Fig. (XI 2a-d). For weakly unstable plasma (larger L_s), the asymptotic field is a very smooth function of space. However, as L_s gets smaller there is a larger and larger discontinuity in derivative at the island edge. Most likely this means that the quasi-linear theory becomes less accurate as the plasma becomes more unstable. The arrow on the horizontal axis of the four graphs is the position of the maximum of $\tilde{B}$ at $\tau = 0$. For weakly unstable plasmas, the final island width turns out to be smaller than this,for strongly unstable plasmas, larger. In Fig. (XI 3) is shown both the final island width and final island width divided by L_s as a function of L_s. In Fig. XI 4 is shown the liberated magnetic energy per unit area and the liberated magnetic energy per unit area

divided by $L_s B_o^2/8\pi$ as a function of scale size. To summarize, the quasi-linear evolution of the outer region always drives a tearing mode to a final stable state with $\Delta = 0$ if one assumes $\langle B_y \rangle$ is linear in x within the inner region. Also, this state will be the same no matter what is the dissipation mechanism in the inner region. However, the quasi-linear theory almost certainly gets less and less accurate as the mode gets more and more unstable.

The next question is whether there are nonlinear effects within the island itself that either stabilize the mode or strongly affect its behavior. This problem was analyzed by Rutherford (P. Rutherford, Phys. Fluids 16, 1903 (1973)). He found that nonlinear effects in the island did not stabilize the mode, but did significantly reduce its growth rate. Here we give a very much simplified version of his theory. To start, recall that Eq. (VII 16) gives the power liberated per unit area in the outer region as

$$P = \frac{\gamma \Delta}{\pi k^2} \tilde{B}_x \frac{d\tilde{B}_x}{dt} \qquad \text{(XI 8)}$$

assuming $\tilde{B}_x$ is real. This power is dissipated by Ohmic heating within the inner region of width L_c. That is, the current associated with the discontinuity in B_y is assumed to flow essentially uniformly within L_c, so that this current is given by Eq. (VII 24), $\tilde{J}_z = \frac{c}{4\pi i k} \tilde{B}_x(x = 0) \frac{\Delta}{L_c}$. Balancing the Ohmic heating with this power liberated yielded the approximate expression for the growth rate, Eq. (VII 25b).

If one now makes the reasonable assumption that for $\Delta x_{is} = 2\left(2\tilde{B}_x \Big/ k \frac{\partial \langle B_y \rangle}{\partial x}\right)^{1/2} > L_c$ the current flows throughout the island, the simple analysis leading up to Eq. VII 25b, is replaced with

$$\frac{d\tilde{B}_x(\rho = \rho_{is})}{dt} = \frac{1}{8} \frac{\gamma c^2}{4\pi} \Delta \left(\frac{\partial \langle B_y \rangle}{\partial x} k \tilde{B}_x \right)^{1/2}, \qquad \text{(XI 9)}$$

or for long time

$$\Delta x_{is} = \frac{1}{4} \frac{\gamma c^2}{4\pi} \Delta t \qquad \text{(X 10)}$$

Thus the island growth becomes linear, rather than exponential in time, and the growth rate goes as first power of resistivity, rather than some fractional power. Thus once $\Delta x_{is} > L_s$, the island growth rate does not stop, but it does drastically slow up, even if Δ does not change. Hence there are two complimentary aspects to the nonlinear evolution of tearing modes. First, as the background evolves, Δ is reduced and eventually brought to zero by the quasi-linear evolution of the outer region magnetic field structure. Second, because of the change in the character of the inner region for $\Delta x_{is} > L_c$, the growth of the island width is drastically reduced and it proceeds on the much slower resistive diffusion time scale, the same time scale as for changes in equilibrium quantities.

Now let us discuss the implication of this for minor and major disruptions in tokamak plasmas. As was discussed in Chapter I, a minor disruption is a sudden burst of x-ray activity generally associated with a measurable disturbance at some m number, usually 2 or 3. The time scale for this x-ray activity in PLT was typically 100 μ sec. One possible interpretation is that tearing modes of the associated helicity are excited. The plasma is not in an absolutely steady state but is continuously evolving due to for instance changes in the external circuit. These changes propagate to the interior of the plasma in a resistive skin time, about 100 miliseconds or more. As the interior of the plasma changes, it might evolve to an unstable state with $\Delta > 0$. Then a tearing mode will be excited. Its growth time will be very small compared to the time for plasma evolution. For PLT, Eq. VII 25b gives a growth time of between about 100 u

sec and 1 milisec depending on which parameters one chooses. The theory developed in this chapter would predict that the plasma then evolves to a stable state at which either $\Delta = 0$ for complete stability, or $\Delta x_{is} \gtrsim L_c$ for drastic reduction in growth rate. The time scale would be several growth times. This would be manifest by the plasma very suddenly changing its equilibrium, accompanied by an x-ray burst and the onset of island structure.

Now let us discuss whether a single tearing mode could lead to a major disruption. Imagine that at some radius a tearing mode is excited. At this radius an island or chain of islands is formed. While the tearing mode evolves quickly compared to the magnetic diffusion time, it evolves slowly compared to the Alfven time. Therefore each of the magnetic surfaces within the island is an MHD equilibrium. Hence as the tearing mode evolves new MHD equilibria form, each flux surface in the island having some average of the pressure of the two or more original flux surfaces which reconnected to form it.

If the island grows to a sufficient size that it touches the limiter, the cold plasma at the limiter will flow freely along the field and end up on the other side of the island, deep in the interior of the plasma. Not only will this cold plasma get to the interior, but in all likelihood large numbers of metal impurity ions from the limiter will also. Radiation from these impurities will further cool the plasma. If the plasma cannot adjust to this sudden cooling of the interior, it may be that a major disruption will result. Thus it is likely that a tearing mode can produce a major disruption in a tokamak if the island can grow until it reaches the limiter. This hypothesis seems to be confirmed by the results on Pulsator discussed

in the introduction. Here an island is artificially induced by external coils, and when the island touches the limiter, a major disruption did result.

This chapter discussed so far how an initially tearing mode unstable plasma in slab geometry evolves toward a final state having a periodic chain of islands. We will close the chapter with a discussion of the subsequent evolution of this island chain. If the original equilibrium variation was in the x direction, this time asymptotic periodic chain of islands extends in the y(horizontal)direction. Each island, of course, represents a current filament in the z direction. Since these currents are all in the same direction, they attract each other. The plasma is in equilibrium because an island feels equal and opposite attractive forces from the island to the right and the island to the left.

Now consider what happens if the island is given a rightward displacement. First of all the attractive force of the two nearby islands is greater than the attractive force to their now more distant neighbors. Thus the nearby islands tend to attract each other and ultimately coalesce so if this effect is dominant, the island chain is unstable. This attractive force, however, may be balanced by a repulsive force. As the two islands move toward each other, the flux, which is frozen into the flow, must be compressed between the two islands. Thus the magnetic pressure increases there and this forces the two islands apart. If this latter effect dominates, the plasma is stable, at least to this type of displacement. The calculation of the stability of this plasma is very complicated due to the two dimensional nature of the equilibrium. One calculation has been made by J. Finn and P. Kaw (Phys. Fluids 20, 72 (1977)) and they found that the attractive force

generally dominate, so that the island chain is unstable to coalescence of the individual islands.

A numerical simulation of the evolution of this equilibrium was done by P. Prichett and C. Wu (Phys. Fluids 22, 2140 (1979)). At t = 0 an MHD equilibrium of a periodic chain of islands was set up, the flux surfaces of which are shown in Fig. (XI 5). The simulation had periodic boundary conditions in the horizontal (y) direction, each periodicity length containing two islands. If the plasma had zero resistivity, the islands displaced toward each other, but ultimately stopped when the magnetic field compressed between them became large enough to repel their coalescing motion. The flux surfaces at two later times are shown in Fig. (XI 6). However, if resistivity is present, the field structure can change its topology and the islands can coalesce. The flux surfaces for a simulation with $\eta \neq 0$ are shown in Fig. (XI 7). Clearly the magnetic reconnection proceeds to completion and the two initial islands merge to form a single island.

Thus the nonlinear evolution of a tearing mode unstable plasma can be quite complex. There are at least three processes which can play a role, quasi-linear evolution of the plasma in the outer region, reduction in growth due to the dynamics of the plasma in the island, and ultimately coalescence of the resulting island chain.

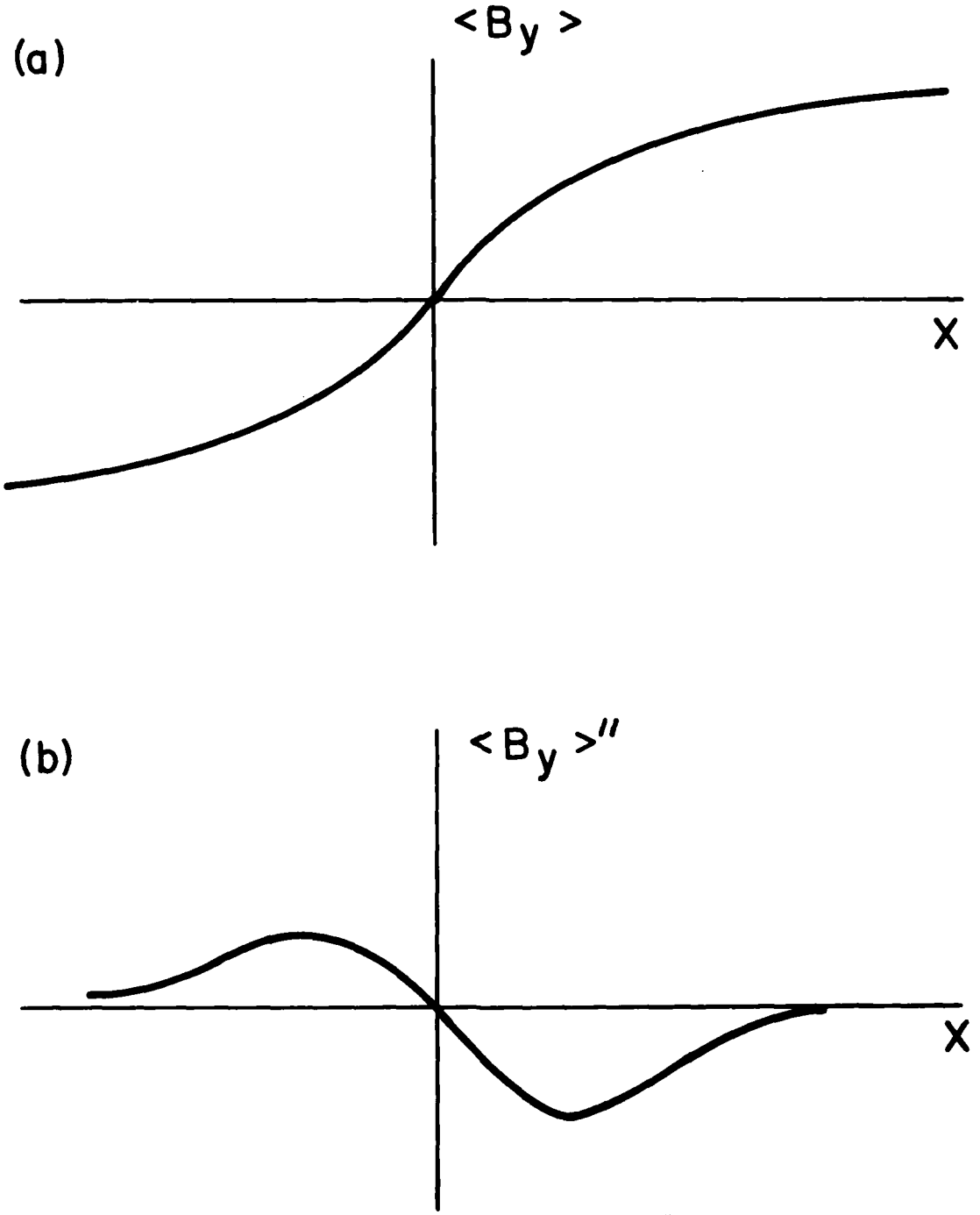

XI 1) The initial profiles of $\langle B_y \rangle$ and $\langle B_y \rangle''$ for a slab plasma unstable to tearing modes

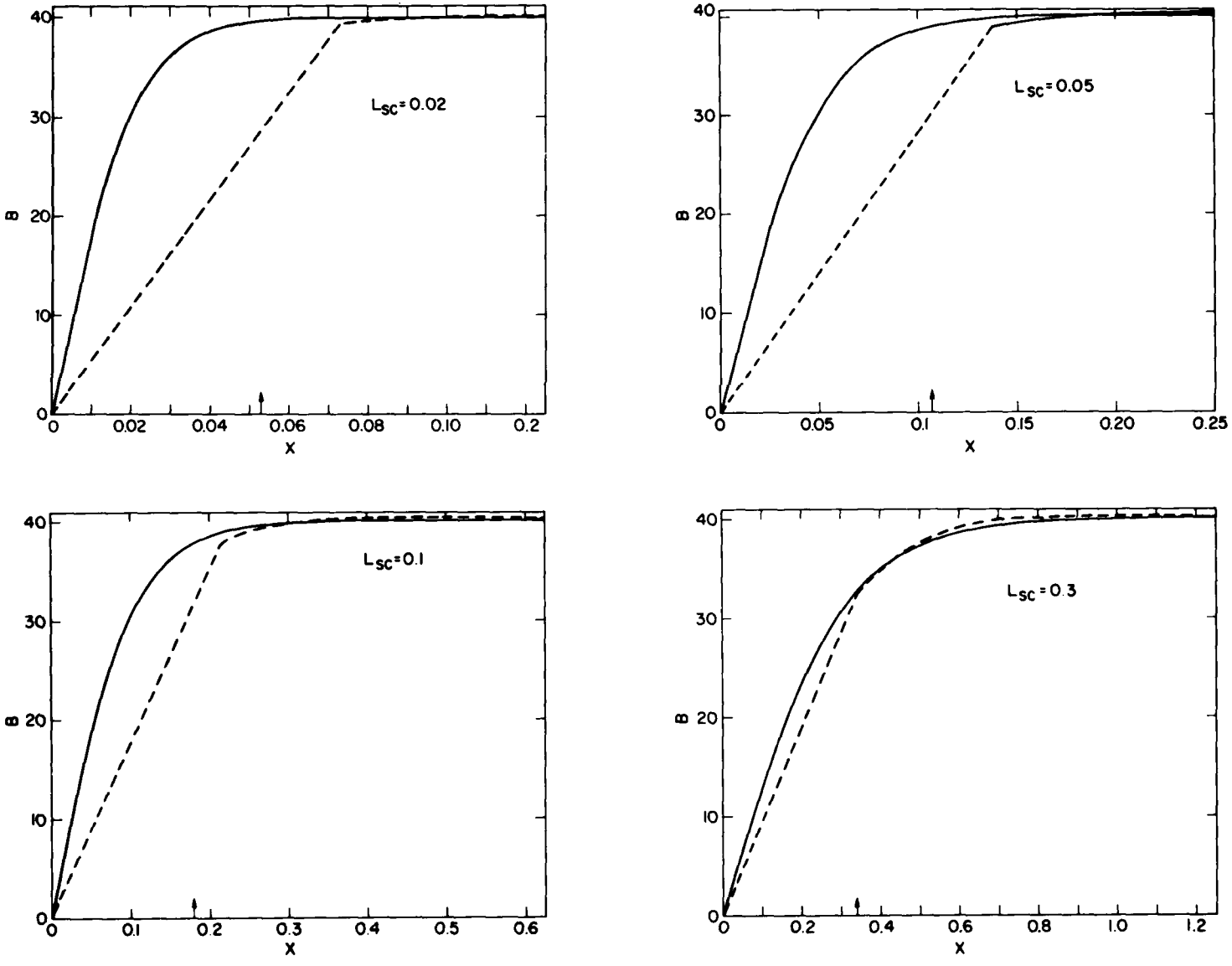

XI 2) The initial (solid) and final (dotted) magnetic field for four scale lengths (scale length normalized to k_y^{-1})

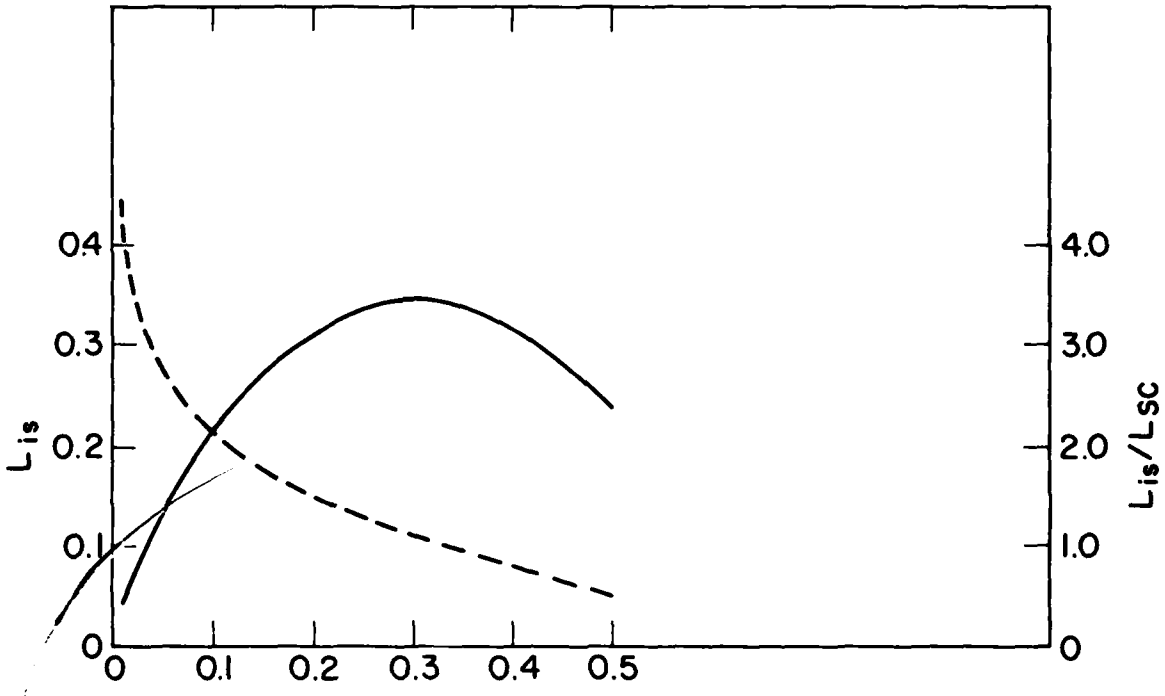

XI 3) The final island width (solid) and final island width divided by initial scale length (dotted) as a function of initial scale length

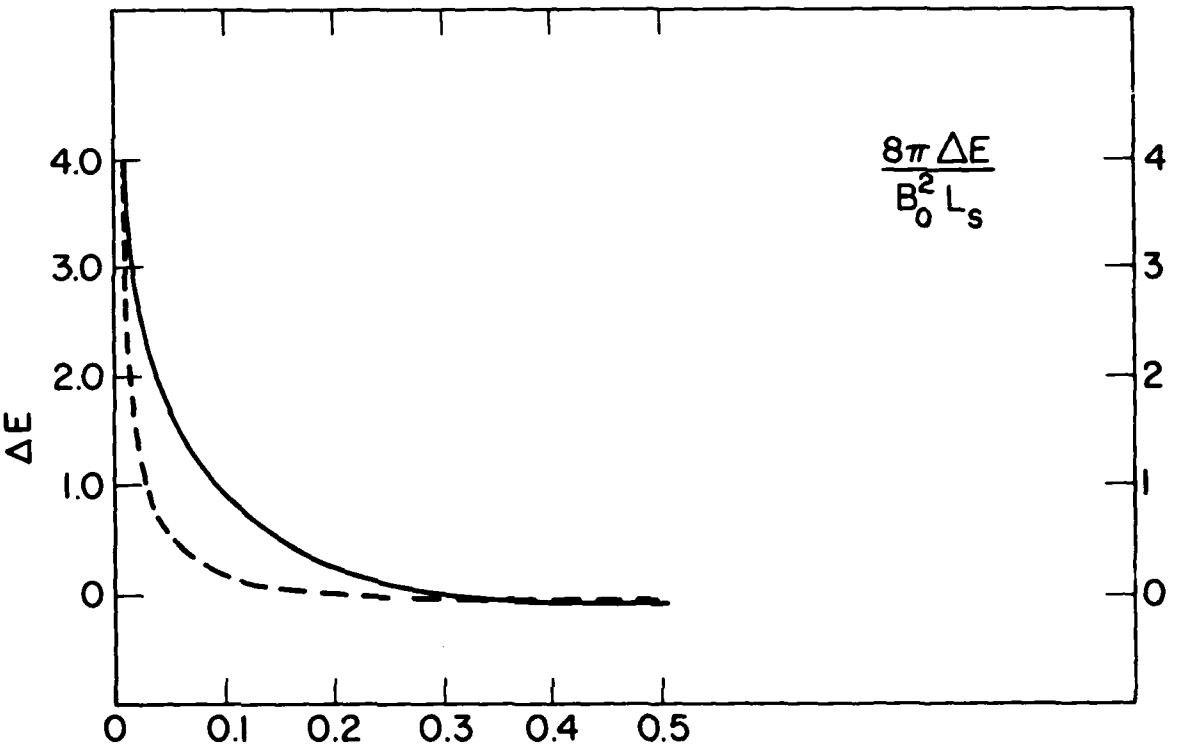

XI 4) Liberated magnetic energy per unit area (solid) and liberated magnetic divided by magnetic energy in a scale length as a function of initial scale length

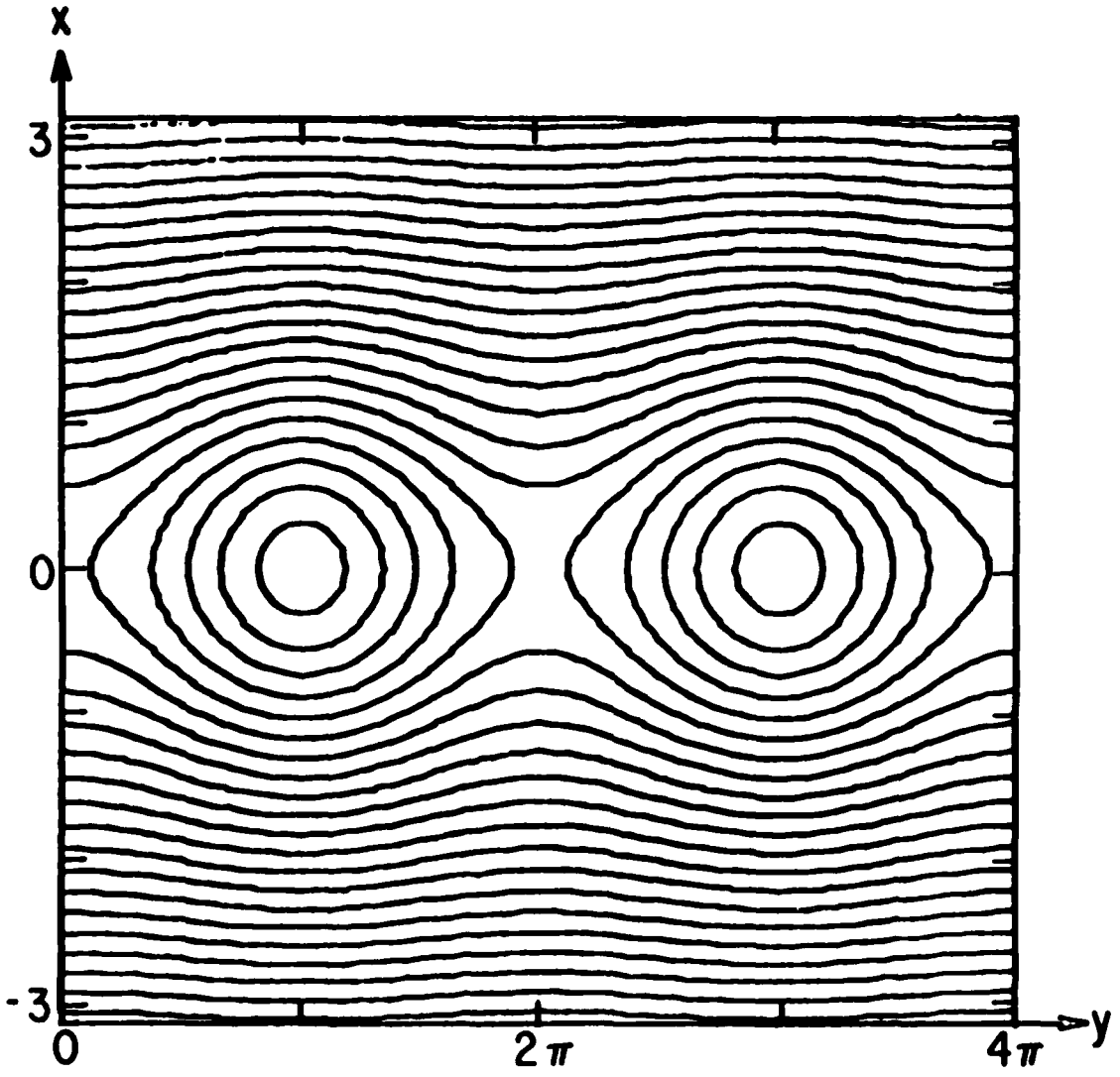

XI 5) The initial island structure examined by Prichett and Wu

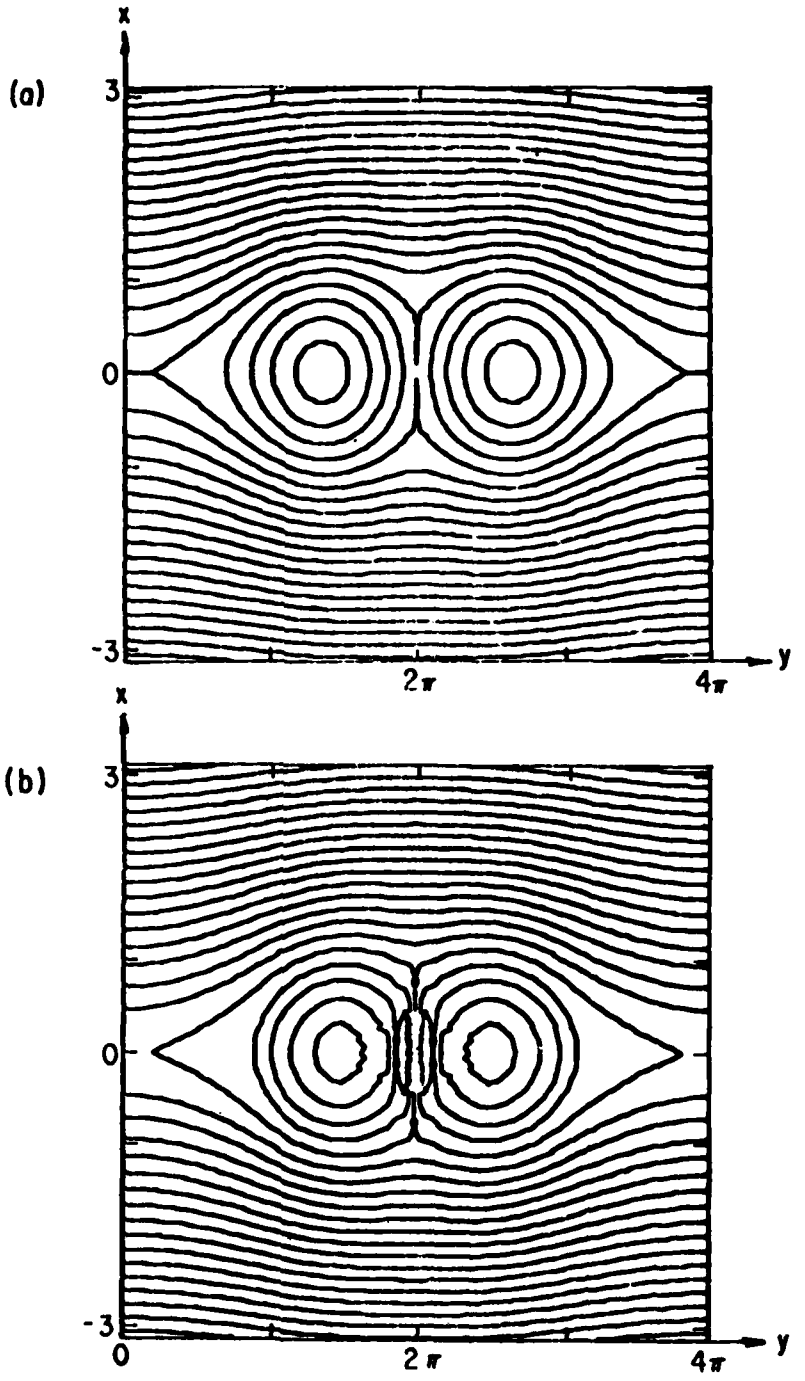

XI 6) The evolution of this island structure for a plasma with $n = 0$

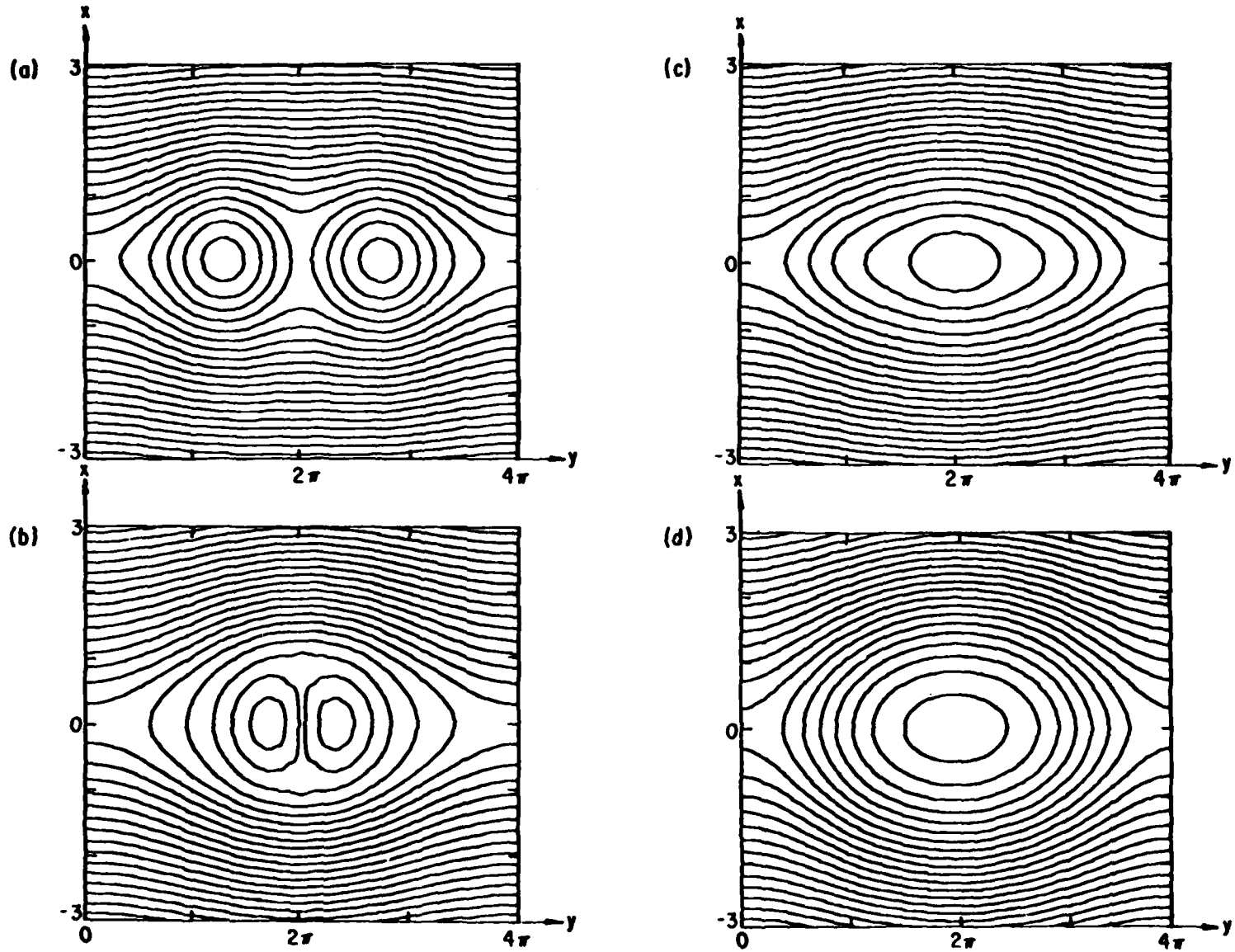

XI 7) The evolution of this island structure for a plasma with $\eta \neq 0$

XII. Island Overlap and the Onset of Stochasticity

In the last chapter we discussed the response of the plasma to a single tearing mode in slab geometry. Although the magnetic topology is changed by a tearing mode, magnetic surfaces still do exist. In this section we investigate under what circumstances unstable MHD fluctuations can destroy magnetic surfaces. For simplicity we consider cylindrical geometry to lowest order in tokamak ordering, so that $\tilde{\underline{B}}$ is two dimensional in r and θ and B_z is constant and very large.

Hence $\underline{B}$ follows from

$$B_r = \frac{1}{r}\frac{\partial}{\partial\theta} A(r,\theta,z) \qquad \text{(a)}$$

$$B_\theta = -\frac{\partial}{\partial r} A(r,\theta,z) \qquad \text{(b)} \qquad \text{(XII 1)}$$

where A is the z component of the vector potential. The equation for the field line is

$$\frac{dr}{dz} = \frac{B_r}{B_z}, \qquad \frac{d\theta}{dz} = \frac{1}{r}\frac{B_\theta}{B_z} \qquad \text{(XII 2)}$$

There are at least two possible ways to display the solution of Eqs. (XII 2). First of all, the solutions could be projected to z = 0, the result being a curve in the $r\theta$ plane. Secondly, if the system is periodic in z with period $2\pi R$ (obviously like a tokamak with radius R), the intersection of the field line with the planes $z = 2\pi nR$ could be displayed on the z = 0 plane. The result now is not a curve, but a series of points which may either lie on a curve, or else fill an area.

Making use of Eq. (XII 1), it is clear that Eqs. (XII 2) are Hamiltonian in form, with z playing the role of t, and A the role of the Hamiltonian. Since A depends on z, the Hamiltonian is not a constant of the motion. However since the motion of the field line does follow from a Hamiltonian,the transformation from $r(z = 0), \theta(z = 0)$ to $r(z), \theta(z)$ is an area preserving transformation. There has been a tremendous amount of recent work on whether such area preserving transformations have an ordered or stochastic nature. (A good introduction and review can be found in J. Ford, Fundamental Problems in Statistical Mechanics III, E. Cohen ed 1974). The basic motivation behind this work is to see when statistical mechanics is valid for an isolated Hamiltonian system. This work can be quite mathematically abstract. For instance it has only recently been proven rigorously that a hard sphere gas obeys the ergodic theorm. To quote Ford, this proof occupies "about one hundred journal pages and will involve such concepts as discontinuous transverse foliations, completely positive Kolmogorov entropy, and the like." Of course it is far beyond the scope of this work to more than scratch the surface of the mathematical theory of ergodic behavior. Principally we are interested in whether the intersection of field lines with $z = 2\pi nR$ (or what we will call the equivalent $z = 0$ plane) fill this plane, or some region of it ergodically, or whether the intersections like on a well defined curve.

One thing is very easy to show. Namely if there does exist a constant of motion say $\chi(r,\theta,z) = \text{constant}$, then the intersections of field lines with the equivalent $z = 0$ plane line on a well defined curve; in other words the motion of the field line is not ergodic. To show this,

first note that since the system is periodic in z,

$$\chi\ (r,\theta,z) = \chi\ (r,\theta,z+2\pi n R) \qquad \text{(XII 3)}$$

Therefore on the equivalent z = 0 plane,

$$\chi\ (r,\theta,z=0) = \text{constant} \qquad \text{(XII 4)}$$

so that the intersections of a field line with this plane lie on the curve defined by Eq. (XII 4).

We will now prove that if the perturbed magnetic field has helical symmetry, that is the dependence on θ and z is through the combination $\tau = m\theta + kz$, then a constant of motion exists. To do so, note that $\underline{\nabla}\cdot\underline{B} = 0$,

$$\frac{\partial}{\partial r} r B_r + m \frac{\partial B_\theta}{\partial \tau} + rk \frac{\partial B_z}{\partial \tau} = 0 \qquad \text{(XII 5)}$$

Therefore B can be expressed in terms of a 'helical flux function' ψ as

$$B_r = -\frac{1}{r}\frac{\partial \psi(r,\tau)}{\partial \tau} \qquad \text{(a)}$$

$$m B_\theta + kr B_z = \frac{\partial \psi(r,\tau)}{\partial r} \qquad \text{(b)} \qquad \text{(XII 6)}$$

The condition that Eqs. (XII 6) have a solution for ψ, if $\underline{B}$ is given, is simply that the divergence of $\underline{B}$ is equal to zero. Notice that in general, Eq. (XII 6) cannot be used to solve for $\underline{B}$ in terms of ψ since it consists of only two equations for the three components of $\underline{B}$. (If tokamak ordering, or B_z = constant, is valid, then Eqs. (XII a and b) also solve for B if ψ is given.) However the information in Eq. (XII 6) is sufficient to show that a constant of motion exists. It follows directly from Eqs. (XII 6) that

$$\underline{B}\cdot\underline{\nabla}\psi = 0 \qquad \text{(XII 7)}$$

so that $\underline{B}$ lies in the surfaces of constant ψ. In other words ψ is constant along the line of force.

Now consider a magnetic field with a helical perturbation specified by

$$\psi(r,z) = \psi_o(r) + \epsilon(r)\cos z \qquad \text{(XII 8)}$$

and for simplicity, take also $k = -\frac{1}{R}$. Note that the derivation of the ψ_o term vanishes at radial position r_s given by

$$q(r_s) = m \qquad \text{(XII 9)}$$

Near this singular surface the surfaces of constant ψ are given by

$$r - r_s = \left(\frac{K - \epsilon(r_s)\cos z}{\frac{1}{2}\psi_o''(r_s)} \right)^{1/2} \qquad \text{(XII 10)}$$

so that the surfaces of constant ψ look as shown in Fig. (XII 1). The maximum radial island (ie when $K = \epsilon$) with, from center to boundary, is given by

$$\Delta r_{is} = 2\left(\frac{\epsilon(r_s)}{\psi_o''} \right)^{1/2} \qquad \text{(XII 11)}$$

returning to standard cylindrical geometry, the surfaces of constant ψ are shown in Fig. (XII 2) for the case of $m = 3$. The projection onto the equivalent $z = 0$ plane is shown in Fig. (XII 3). Thus for the case of a single perturbation, the helical symmetry allows us to prove the existence of constant of motion. Therefore the field line is not ergodic.

The obvious question next is what happens if the helical symmetry is broken, for instance by the presence of an additional perturbation with k still equal to $-\frac{1}{R}$ but a different asimuthal wave number m'. Now there is no single helical symmetry, and apparently no constant of motion. This problem has been investigated extensively by numerical simulation. While a fact of ergodicity still eludes a rigorous mathematical proof, the results of many numerical simulations and analytic theories does point toward a very

reasonable hypothesis. Namely, if the island widths of the m and m′ perturbation are small compared to the inter-island separation, well define islands exist around the q = m and q = m′ points. However the separatrices may not be distinct lines but rather thin ergodic regions. Between the q = m and q = m′ points, the field line projections are mostly as in Fig. (XII 3) except there may be small regions of ergodicity and small chains of secondary islands, as indicated in Fig. (XII 4a) for an m = 2 and m = 3 perturbation with all islands having the same width. As the island width increases, the ergodic regions increase around the separatrix as shown in Fig. (XII 4b). Finally, when the island edges overlap, most of the region between the q = 2 and q = 3 surface is ergodic, except for perhaps a small region in the center of each island, as shown in Fig. (XII 4c). Thus the condition of island overlap is almost universally accepted to be the condition for ergodic behavior between the relevant rational surfaces.

Let us see what this implies for the case of a m = 2 and m = 3 perturbation. The distance between the two rational surfaces q = 2 and q = 3 is given roughly by

$$\Delta r_{rat} \approx \left(\frac{\partial q}{\partial r}\right)^{-1} \qquad \text{(XII 12)}$$

while the island width is given by Eq. (XII 11). Expressing χ_0'' in terms of $\frac{\partial q}{\partial r}$, we find

$$\Delta r_{is} \approx 2\left(\frac{\epsilon}{B_\theta q'}\right)^{1/2} \qquad \text{(XII 13)}$$

assuming $\epsilon(m = 2) = \epsilon(m = 3)$. Hence an approximate condition for island overlap is

$$\epsilon > \frac{1}{16} B_\theta \Big/ \left(\frac{\partial q}{\partial r}\right) \qquad \text{(XII 14)}$$

Thus in a system with strong shear (large q'), island overlap is accomplished with smaller perturbed field. Each island width is smaller, but the distance between neighboring rational surfaces is also less.

Consider now the implication of this for a tokamak plasma. Imagine that the plasma is initially unstable to both an $m = 2$ and $m = 3$ tearing mode. In the early stages, when the island width is small compared to island separation, the equilibrium must readjust to the presence of the fluctuations, but since magnetic surfaces exist, equilibrium also at least exists. However when the perturbations grow to such an amplitude that these islands overlap MHD equilibrium is suddenly (ie within a growth time) lost in a very large region of the plasma, and the only possible pressure profile is p = constant in this extensive ergodic region. If this sudden and violent re-arrangement of the pressure profile is sufficient to cause a major disruption of a tokamak discharge, then island overlap is one possible cause of such major disruptions.

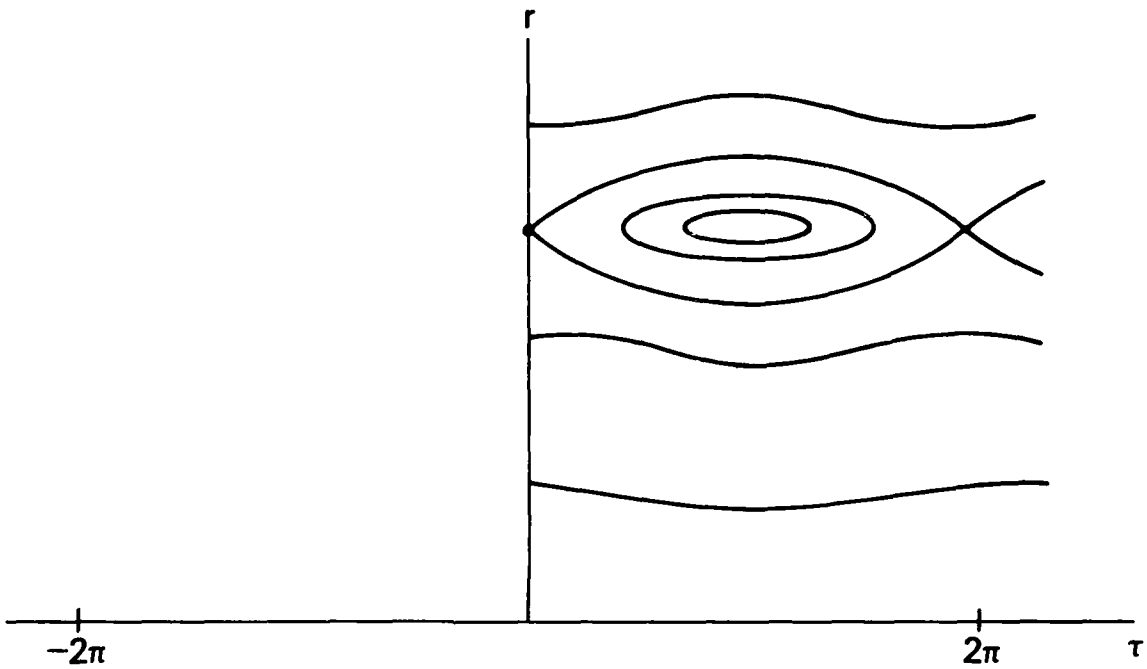

XII 1) A plot of ψ as a function of τ

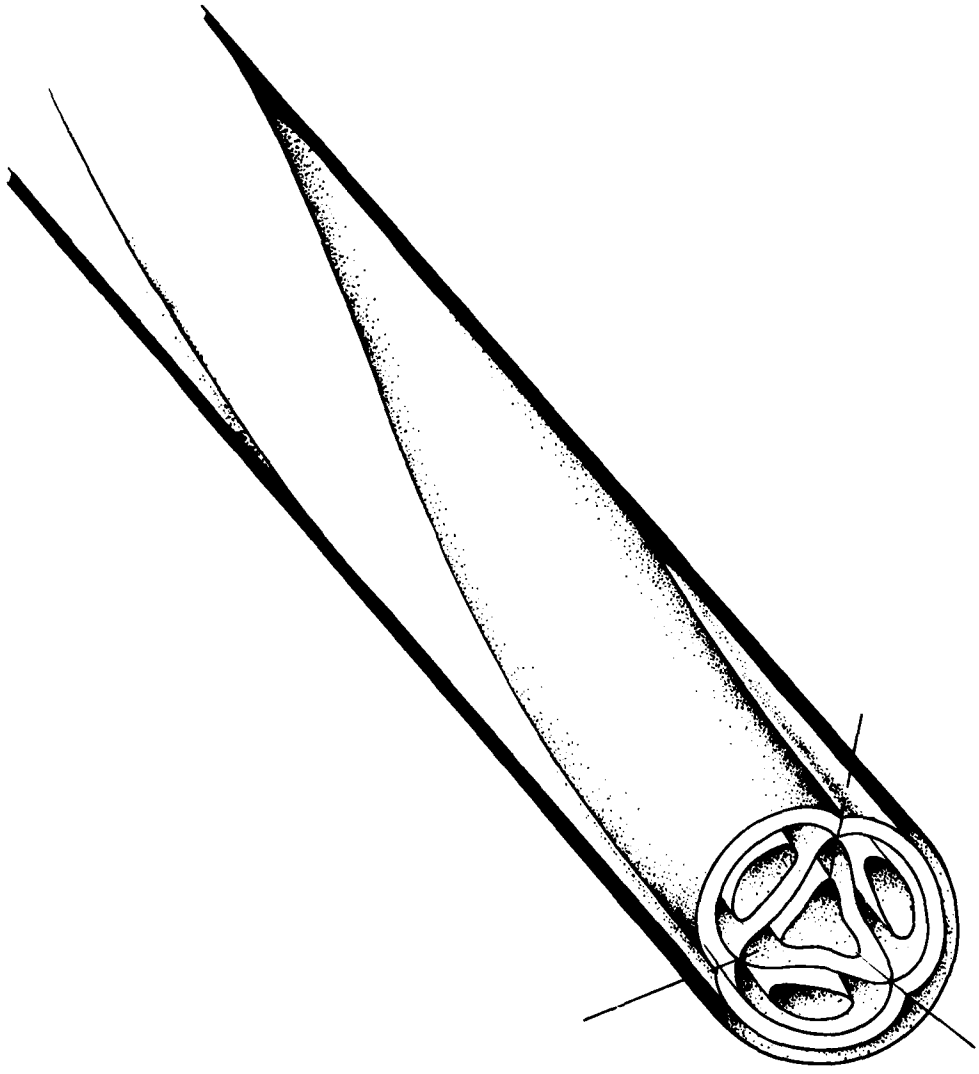

XII 2) The island structure in cylindrical geometry for m = 3

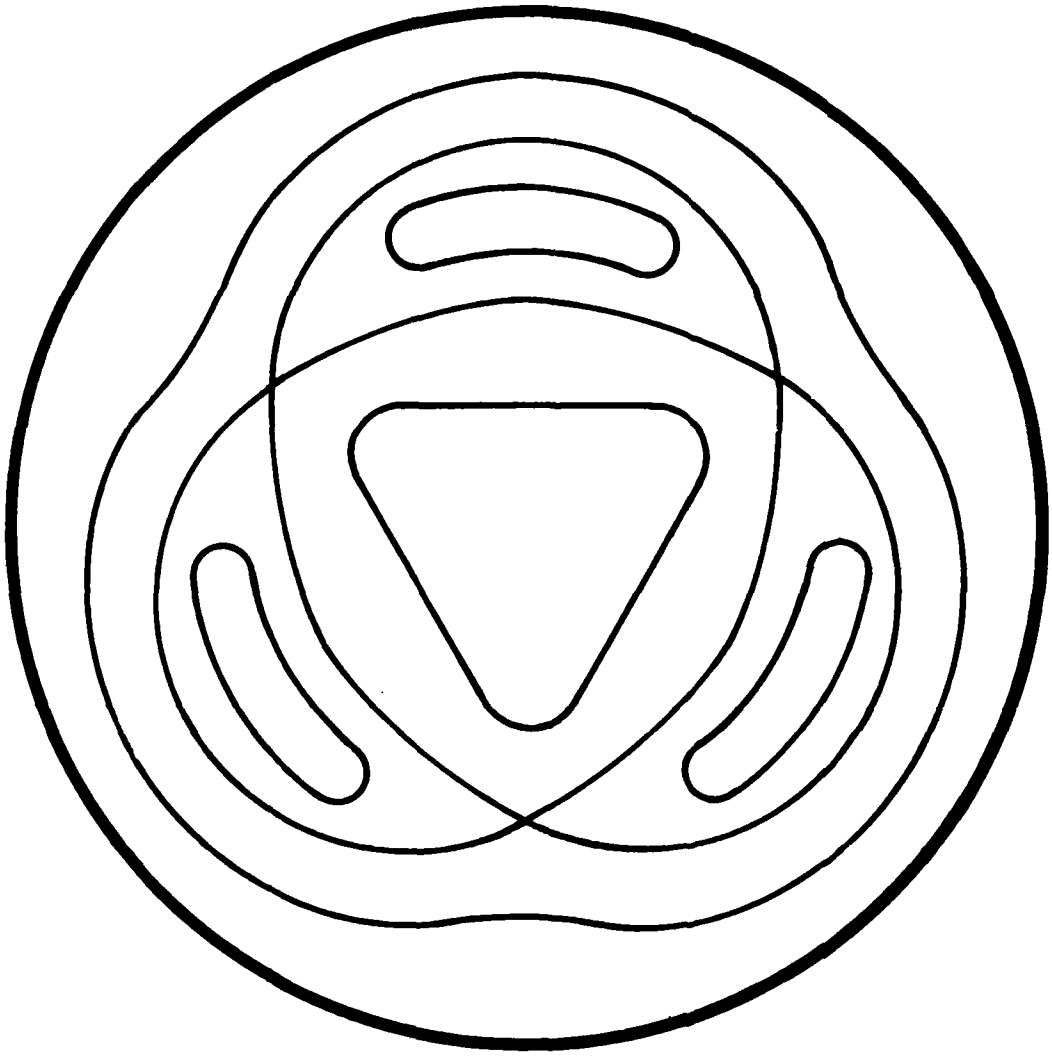

XII 3) The projection of the island structure onto the equivalent Z = 0 plane for m = 3

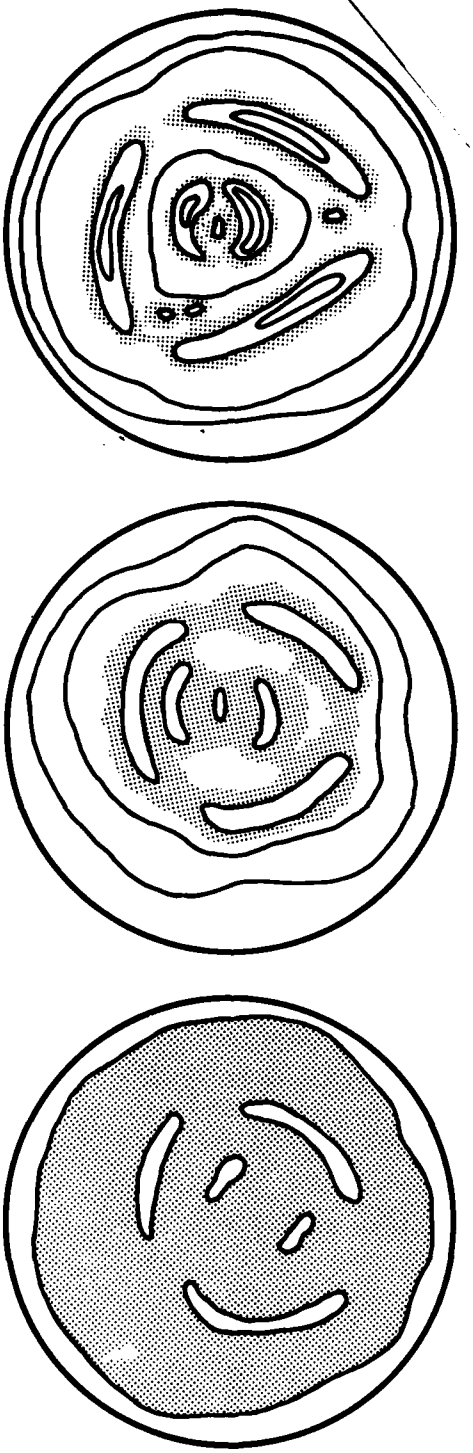

XII 4) The projection of the island structure onto the equivalent Z = 0 plane for the case of equal m = 2 and m = 3 perturbations. The dotted regions represent the region of stochastic field lines. As the amplitude of the perturbations increase, more of the region is stochastic.

XIII. The Taylor-Woltjer Theory of Spontaneous Field Reversal and Current Limitation

The past three chapters have discussed nonlinear theory with reference to some particular instability. Other authors, however, have looked at the nonlinear motion of an unstable plasmas, but without specific reference to a particular instability. In this chapter and the next, we survey some of this work. This chapter discusses the theory of Woltjer (Proc. Natl. Acad. Sci. U.S. 44, 489 (1958))and Taylor (Phys. Rev. Lett. 33, 1139 (1974)), for spontaneous reversal of the axial field and of current limitation in a reversed field pinch. The fundamental assumption in this work is that a plasma will relax to its lowest energy state consistent with all the constraints on it. Taylor's main initial assumption is that the thermal and flow energy of the plasma is much less than the magnetic energy, $\int d^3r\, B^2/8\pi$. This (unfortunately) is true in current tokamaks and pinches, although the ultimate hope is certainly to attain a high beta plasma. The fact that the pressure is vanishingly small, of course, imposes severe constraints on the MHD equilibrium. Consider for a moment the MHD equilibrium of a high aspect ratio ($R/a \gg 1$) torus; that is the topology is that of a torus, but all vector equations can be expressed in cylindrical co-ordinates. This equilibrium now becomes

$$\frac{1}{4\pi}(\nabla \times \underline{B}) \times \underline{B} = \nabla p = 0 \qquad \text{(XIII 1)}$$

Equation (XIII 1) simply says that ∇ x $\underline{B}$ is everywhere parallel to $\underline{B}$, or

$$\nabla \times \underline{B} = \lambda(r)\underline{B} \qquad \text{(XIII 2)}$$

where λ is some scalar function of position. Taking the divergence of both sides of Eq. (XIII 2) and making use of the fact that $\nabla \cdot B = 0$, we find

$$B \cdot \nabla \lambda = 0 \qquad \text{(XIII 3)}$$

so that λ is constant along every flux tube, flux surface, or flux volume; whichever is appropriate.

Taylors theory then gives a prescription for finding λ and also determining the resulting boundary conditions for Eq. (XIII 2). It does this by minimizing the magnetic energy subject to appropriate constraints. The first order of business then is to find these constraints; minimizing magnetic energy subject to no constraints gives only the trivial solution $\underline{B} = 0$.

The configuration is a toroidal pinch bounded by a conductor. However, as shown in Fig. (XIII 1), there is a poloidal slit with a voltage source across it. At $t = 0$, $\underline{J} = 0$ and there is only a toroidal field specified by

$$\underline{B} = B_i \underline{i}_z \qquad A = \frac{r B_i}{2} \underline{i}_\theta \qquad \text{(XIII 4)}$$

Then at $t = 0$, a voltage V_o is pulsed across the gap for a time δt. For later times, the gap is shorted out (crowbarred). The plasma then responds to this induced voltage, and relaxes, presumably due to instabilities, to some final minimum energy state. Since the plasma is surrounded by a perfect conductor, no toroidal flux can get in or out, so the toroidal flux is conserved and has value $\Psi = \pi B_i a^2$. However because of the poloidal slit, poloidal flux can go in or out during the time δt, so it is not conserved. Thus the first constraint is that Ψ is constant. As we will see, this determines the boundary conditions.

A second constraint follows from the fact that the magnetic flux is frozen into the fluid flow. We will now show that this implies that as the fluid relaxes, $K = \int \underline{A} \cdot \underline{B} d^3r$ is constant after the voltage pulse is shut off. Since $\underline{B} = \nabla \times \underline{A}$, Maxwell's equation for $\partial \underline{B}/\partial t$ (Eq. II 8) can be integrated once to give

$$\frac{\partial \underline{A}}{\partial t} - \nabla \times \underline{B} = \nabla \varphi \qquad \text{(XIII 5)}$$

where φ is any scalar function. The presence of φ on the right hand side of Eq. (XIII 5) of course accounts for the guage. Taking the dot product of Eq. (XIII 5) with $\underline{B}$ and integrating over space gives the result

$$\iiint d^3r\, \underline{B}\cdot\frac{\partial \underline{A}}{\partial t} = \iiint d^3r\, \underline{B}\cdot\nabla\varphi = \oiint d\underline{S}\cdot\underline{B}\,\varphi = 0 \qquad \text{(XIII 6)}$$

The surface integral arises because $\nabla\cdot B = 0$; it vanishes because $\underline{B}$ is everywhere normal to the bounding surface. Thus

$$\frac{d}{dt}\iiint d^3r\, \underline{B}\cdot\underline{A} = \iiint d^3r\, \underline{A}\cdot\frac{\partial \underline{B}}{\partial t} = c\iiint d^3r\, \underline{A}\cdot\nabla\times\underline{E}$$

$$= c\left\{\iiint E\cdot B\, d^3r - \oiint d\underline{S}\cdot(\underline{A}\times\underline{E})\right\} \qquad \text{(XIII 7)}$$

Now examine the two terms on the extreme right hand side of Eq. (XIII 7). In a perfectly conducting plasma $\underline{E}$ is perpendicular to $\underline{B}$, so the first term vanishes. To evaluate the second, we need the components of $\underline{E}$ and $\underline{A}$ only in the plane of the bounding surface. After the system is crowbarred, $\underline{E}$ is zero in the plane of the surface (since the surface is a perfect conductor), so that $\iiint d^3r\, A\cdot B$ is constant.

For the time δt, during which the system is pulsed, $E_z = V_o/\delta$ is the width of the slit, so that

$$c\oiint(\underline{A}\times\underline{E})\cdot d\underline{S} = c\int_0^{2\pi} a\, d\theta\int_0^{\delta} dz\ \frac{-V_o}{\delta}\, A_\theta \qquad \text{(XIII 8)}$$

Thus the rate of change of K is simply proportional to the product of voltage times toroidal flux. Since K (t = 0) = 0, as is obvious from Eq. (XIII 4), then

$$K = \iiint \underline{A}\cdot\underline{B}\, d^3r = -\,cV_o\,\delta t\,\Psi \qquad \text{(XIII 9)}$$

so that after time δt, K is proportional to the Volt-seconds stored in the external circuit.

The problem now is to determine the state that the plasma relaxes to after the voltage source is turned off. The basic assumption is that the plasma relaxes (presumably by instability) to a state which minimizes the magnetic energy, subject to the constraint that K is constant. Using the method of Lagrange multipliers, this means minimizing

$$\iiint \left(B^2 - \mu \, \underline{A}\cdot\underline{B}\right) d^3r \qquad \text{(XIII 10)}$$

where μ is the Lagrange multiplier. It is a simple matter to show that the right hand term in Eq. (XIII 10) is guage invariant by letting $\underline{A} \to \underline{A} + \underline{\nabla}\varphi$, integrating by parts, and making use of the fact that $\underline{B}$ is parallel to the surrounding conducting wall. To minimize the expression in Eq. (XIII 10), let $\underline{B} \to \underline{B} + \delta\underline{B}$, $\underline{A} \to \underline{A} + \delta\underline{A}$ (of course $\delta\underline{B} = \underline{\nabla} \times \delta\underline{A}$), and set terms linear in $\delta\underline{A}$ and $\delta\underline{B}$ equal to zero, so that

$$\iiint d^3r \left[2\underline{B}\cdot\delta\underline{B} - \mu\left(\delta\underline{A}\cdot\underline{B} + \underline{A}\cdot\delta\underline{B}\right)\right] = 0 \qquad \text{(XIII 11)}$$

Writing $\underline{B}$ and $\delta\underline{B}$ in terms of $\underline{A}$ and $\delta\underline{A}$ and performing various partial integrations, it is not difficult to show that Eq. (XIII 11) reduces to

$$2\iiint d^3r \, \delta\underline{A}\cdot\left[\underline{\nabla}\times\underline{B} - \mu\,\underline{B}\right] + \oiint \left\{2\underline{B} - \mu\underline{A}\right\}\times\delta\underline{A} = 0 \qquad \text{(XIII 12)}$$

where the second integral in Eq. (XIII 12) is over the bounding conducting surface. The next step is to prove that this surface integral vanishes.

To start, consider the integral $\oint \underline{A}\cdot d\underline{\ell}$ around any closed curve on the surface. This integral is just the magnetic flux linking the closed curve.

There are two possibilities. If the curve links the torus in the poloidal direction, the integral is Ψ, the toroidal flux. Otherwise the integral vanishes. Since all variations in $\underline{B}$ leave the flux invariant,

$$\oint \delta\underline{A} \cdot d\underline{\ell} = 0 \qquad \text{(XIII 13)}$$

Therefore on the bounding surface $\delta\underline{A} = \underline{\nabla}_s g$ where $\underline{\nabla}_s$ is a two dimensional gradient within the surface, and g is a scalar function defined on the surface. Since $\delta\underline{A}$ normal to the surface gives no contribution to the second term in Eq. (XIII 12), it can be written as

$$\oiint \{(2\underline{B} - \mu\underline{A}) \times \underline{\nabla}_s g\} \cdot d\underline{S} = \oiint g\, \underline{\nabla} \times (2\underline{B} - \mu\underline{A}) \cdot d\underline{S} - \oiint \underline{\nabla} \times g(2\underline{B} - \mu\underline{A}) \cdot d\underline{S} \qquad \text{(XIII 14)}$$

The second term on the right of Eq. (XIII 14) vanishes since the integral over a closed surface of the curl of any vector vanishes. The first term can be expressed as

$$\oiint g\, \underline{\nabla} \times (2\underline{B} - \mu\underline{A}) \cdot d\underline{S} = \oiint g \left(\frac{8\pi}{c}\underline{J} - \mu\underline{B}\right) \cdot dS \qquad \text{(XIII 15)}$$

Because the normal component of both $\underline{J}$ and $\underline{B}$ are equal to zero on the conducting surface, the right hand side of Eq. (XIII 15) is zero. Hence setting the constrained variation of energy equal to zero, Eq. (XIII 12) reduces to the simple result

$$\underline{\nabla} \times \underline{B} = \mu\underline{B} \qquad \text{(XIII 16)}$$

Comparing Eq. (XIII 16) to Eq. (XIII 2) we see that the only difference is that μ is a constant, whereas λ is constant over a flux tube or surface, but otherwise can vary in space. Thus minimizing the energy subject to the constraint K = constant, picks out a particular

MHD equilibrium out of all those which are possible according to Eq. (XIII 2). Let us now examine how this selection comes about.

In deriving Eq. (XIII 16), the only boundary conditions used were that the components of $\underline{B}$ and $\underline{J}$ normal to the conducting surface both vanish. In ideal MHD, this is not only true at the conducting wall, but is also true of each flux surface, as shown in Chapter II. Therefore, one could equally well minimize the magnetic energy between two flux surfaces, subject to the constraint that K is constant, between them, and derive Eq. (XIII 2) in exactly the same way as Eq. (XIII 16) was derived. Imagine that at $t = 0$ the flux surfaces are circular, as shown in Fig. (XIII 2a), but $\underline{\nabla} \times \underline{B} \neq \lambda(\Psi)\underline{B}$ (Ψ denotes the flux). As the plasma releases its excess magnetic energy and violently evolves toward a final state described by Eq. (XIII 2), these flux surfaces will naturally become very contorted, but must maintain their topological structure because the flux is frozen into the flow, as discussed in Chapter II. For instance at $t = \infty$ infinity, these three flux surfaces might evolve toward that shown in Fig. (XIII 2b). In this final state $\underline{\nabla} \times \underline{B} = \lambda(\Psi)\underline{B}$ on each flux surface, but λ can vary from one flux surface to another. Notice that there are places in Fig. (XIII 2b) where flux surfaces are forced together. For instance at the star, all three flux surfaces are forced together. Of course all flux surfaces initially between 1 and 3 are forced together at this point also.

Now imagine that there is a very small plasma resistivity, so that the field lines can reconnect. For instance if resistivity were suddenly turned on for the configuration in Fig. (XIII 2b), surely all flux surfaces between 1 and 3 would reconnect with one another near the star, and other reconnection would occur at other places also. Of course reconnection changes topology of $\underline{B}$, but only has a small effect on the magnitude of B in most places.

Therefore, if this reconnection is allowed, it makes no sense to talk about magnetic energy or constraints between two flux surfaces! However all relevant boundary conditions can still be applied on the conducting wall, so that minimizing the total plasma energy, subject to the constraint that K is constant is still valid for the entire plasma even if not for each initial flux surface. Thus inherent in the reduction of Eq. (XIII 2) (which could have also been derived by minimizing the energy on each flux surface) to Eq. (XIII 16) is the assumption that in the violent relaxation of the plasma to its final state, a small amount of resistivity is allowed, so that topology of the field is destroyed.

Now let us find the solution to Eq. (XIII 16). If $\underline{B}$ has cylindrical symmetry, it is a simple matter to show that

$$B_z = B_0 J_0(\mu r)$$
$$B_\theta = B_0 J_1(\mu r) \qquad \text{(XIII 17)}$$

is a solution of Eq. (XIII 17), and

$$A_z = \frac{B_0}{\mu}\left[J_0(\mu r) - J_0(\mu a)\right]$$
$$A_\theta = \frac{B_0}{\mu} J_1(\mu r) \qquad \text{(XIII 18)}$$

Here a is the minor radius and A_z has an appropriate constant added to it so that the poloidal magnetic flux through the hole in the torus vanishes. The next problem is to relate μ and B_0 to physical parameters. The axial magnetic flux Ψ is just the line integral of the poloidal vector potential, so

$$\Psi = \frac{2\pi a}{\mu} J_1(\mu a) \qquad \text{(XIII 19)}$$

The simplest other relation is that between μ and the pinch ratio $2I/aB_1c$ where B_1 is the initial axial bias field at time t = 0. Relating

B_i to the flux Ψ, and the current to B_θ (r = a), we find

$$\frac{a^2 I}{a B_i c} = \frac{\mu}{2} \qquad \text{(XIII 20)}$$

where I is the current in CGS units. The quantity K is related to the stored Volt seconds by Eq. (XIII 9). Using the expression for the fields given in Eq. (XIII 17 and 18), one can show that

$$\frac{K}{\Psi^2} = \frac{R}{a}\left[\frac{\mu a\left(J_0^2(\mu a) + J_1^2(\mu a)\right) - 2 J_0(\mu a) J_1(\mu a)}{J_1^2(\mu a)}\right] \qquad \text{(XIII 21)}$$

which defines μ in terms of initial flux and stored Volt seconds.

The remarkable thing about Eq. (XIII 17) is that it predicts that the toroidal field reverses direction whenever $\mu a > 2.4$, the position of the first zero of J_0, or for pinch parameter

$$\frac{a^2 I}{a B_i c} > 1.2 \qquad \text{(XIII 22)}$$

This is in reasonable agreement with the results of pinch experiments as shown in Eq. (I).

So far, we have only considered solutions of Eq. (XIII 16) which have cylindrical symmetry. These are also solutions which are not symmetric. Expressing the azimuthal and axial dependence of the non-symmetric solution to Eq. (XIII 16) as exp i(kz + mθ), and using $\nabla \cdot B = 0$, it is not difficult to show that B_z satisfies Bessels equation, so that the solutions are

$$B_z = J_m(y)\cos(m\theta + kz)$$

$$B_r = \frac{-1}{(\mu^2 - k^2)^{1/2}}\left\{k J_m'(y) + \frac{m\mu}{y} J_m(y)\right\}\sin(m\theta + kz) \qquad \text{(XIII 23)}$$

$$B_\theta = \frac{-1}{(\mu^2 - k^2)^{1/2}}\left\{\mu J_m'(y) + \frac{mk}{y} J_m(y)\right\}\cos(m\theta + kz)$$

with $y^2 = (\mu^2 - k^2)r^2$. Of course Eq. (XIII 23) is only a valid solution to the equation if

$$B_r(r=a) = 0 \tag{XIII 24}$$

This then imposes a relation between μ and k which must be satisfied.

Since Eq. (XIII 16) is linear, the magnetic field can be the symmetric state, Eq. (XIII 17), plus any linear combination of individual solutions in Eq. (XIII 23). The condition this solution must satisfy is that the total K and toroidal flux is given and that $B_r(r = a) = 0$. Since the solutions given in Eq. (XIII 23) have zero toroidal flux, this toroidal flux is determined entirely by the symmetric state. The quantity K then is a summation over contributions from each solution in Eq. (XIII 23) plus the contribution from the symmetric state.

The question now is which state the plasma picks out. Of course the state is that having minimum magnetic energy. Imagine now that there are two solutions to Eq. (XIII 16) having two different values of μ and which satisfy all of the appropriate boundary conditions. We now show that the minimum energy state is the state having minimum μ. The energy is given by

$$W = \iiint d^3r\, \underline{B} \cdot \underline{B} = \iiint d^3r\, \underline{B} \cdot \underline{\nabla} \times \underline{A} \tag{XIII 25}$$

Writing $\underline{B}$ in terms of $\underline{A}$ in Eq. (XIII 16) and integrating once, it is easy to show that

$$\underline{\nabla} \times \underline{A} = \mu \underline{A} + \underline{\nabla} \varphi \tag{XIII 26}$$

where φ is any scalar function. Thus

$$W = \iiint \underline{B} \cdot (\underline{\nabla} \varphi + \mu \underline{A}) d^3r = \mu K \tag{XIII 27}$$

The φ term vanishes, as one can show by integrating it by parts. Therefore, since K is constant, the minimum energy state is the state with minimum μ.

One possible state for the plasma is simply the symmetric state of Eq. (XIII 17). However if a helically perturbed state with smaller μ can be found, the plasma should relax to it. Taylor (J. B. Taylor, Plasma Physics and Controlled Fusion Research, 1975, IAEA Vienna) has performed a detailed investigation and found that the smallest μ for which Eq. (XIII 24) can be satisfied is $\mu a = 3.11$ for a helical perturbation having $m = 1$ and $ka = 1.25$. Since all other helical states have higher μ, and higher energy, we need only consider this one.

Now review how the plasma state is set up. At $t = 0$, there is some toroidal flux and the system is pulsed with a certain number of volt-seconds (ie K). A current (proportional to μ) is thereby induced in the plasma. The natural expectation is that I (or equivalently μ), is a monotonically increasing function of K (the volt seconds). However for a sufficiently large K, μ will be equal to 3.11. As K is further increased the current will no longer increase. The reason is that a lower energy state exists which is a linear combination of the cylindrically symmetric state and helical state with $\mu = 3.11$. The toroidal flux is determined by the cylindrical state, and the relative amplitudes of the cylindrical and helical state are specified by K. Thus after $\mu = 3.11$, increasing the Volt seconds does not increase the current, but rather increases the amplitude of the helical displacement. The current limitation predicted here,

$$\frac{\alpha I}{a B_i c} = 1.56 \qquad \text{(XIII 28)}$$

is also in reasonable agreement with what is measured in pinch experiments, as given in Eq. (I). Thus this relatively simple theory gives quite

good agreement with experiment on the two really amazing features of reverse field pinches, spontaneous field reversal and current limitation.

To conclude, it is worth noting that Gibson and Whiteman (Plasma Phys. 10, 1101 (1968))have examined the stability of the cylindrically symmetric state to tearing modes. They have shown that this transition from a cylindrically symmetric state to a helically perturbed state corresponds to the marginally stable point. Of course this is to be expected, since as was shown in Chapter VII, the tearing mode first goes unstable when the magnetic structure has a neighboring equilibrium at the same energy. The theory in this chapter however is quite different from linear stability theory in that growth rates are not calculated, but the amplitude of the helical perturbation is.

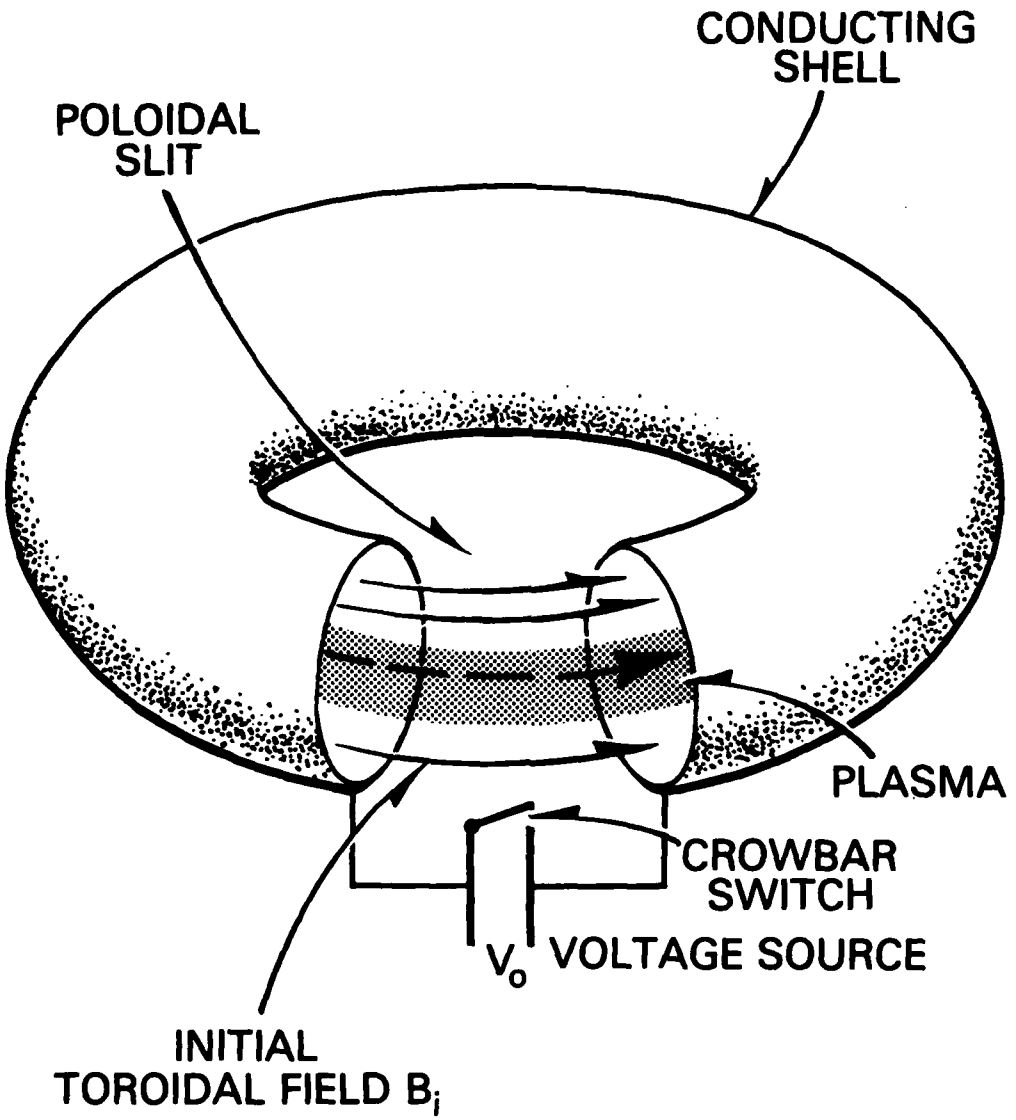

XIII 1) A Schematic of a Reverse Field Pinch

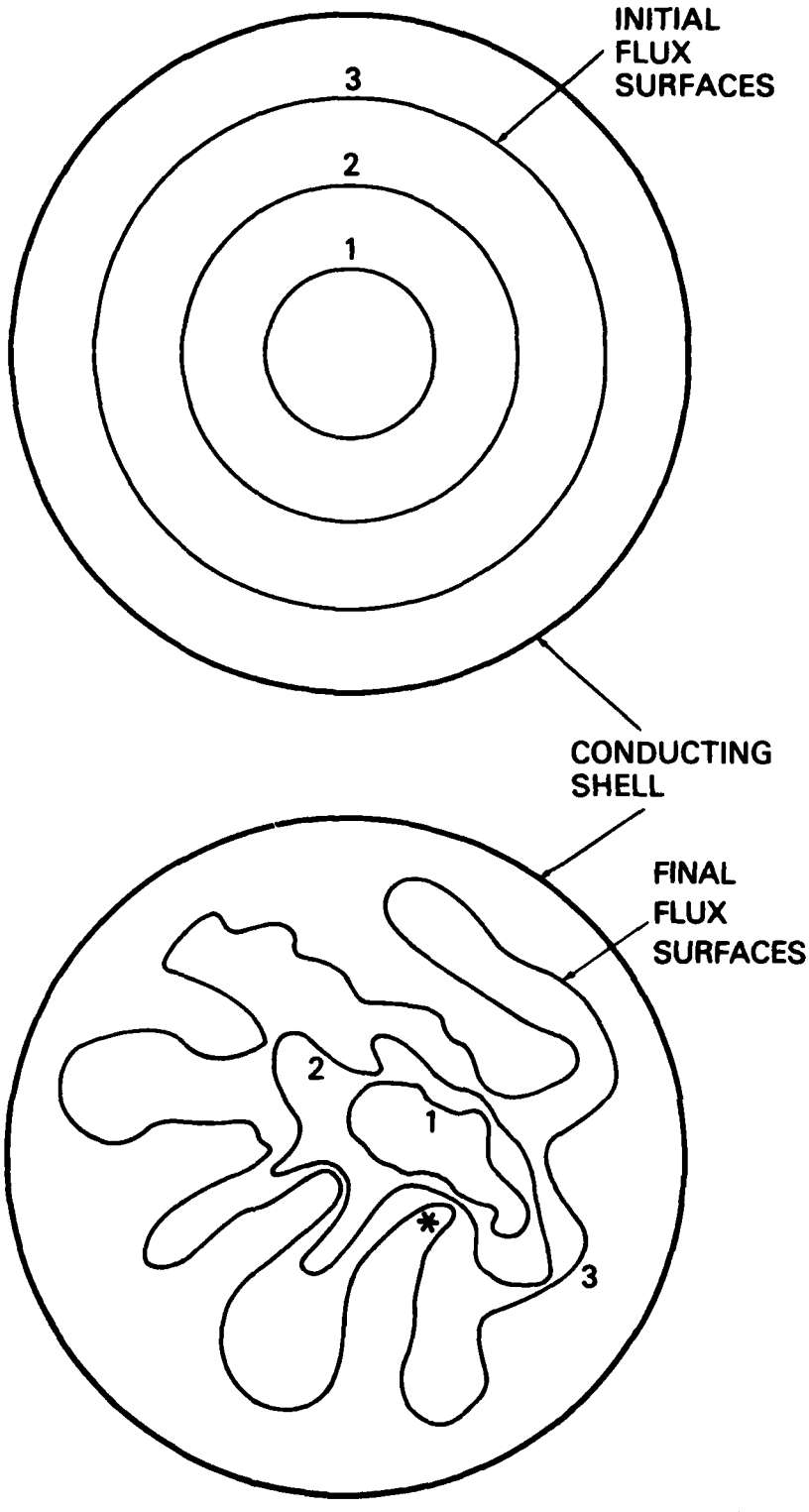

XIII 2) Schematics of initial flux surfaces and final flux surfaces having $\nabla \times B = \mu B$. Note that because of the ideal MHD constraint, the topology is preserved.

XIV. Kadomtsev's Theory of Internal Disruptions and Introduction to Numerical Simulations

This final chapter begins with Kadomtsev's theory for m = 1 internal disruptions in a tokamak. Amazingly enough, he is able to develop this theory without ever getting involved in the complications of the m = n = 1 internal kink-tearing mode. Preliminary to discussing this theory, it is necessary to review the toroidal flux ψ first introduced in Chapter XII. Since all dependence on θ occurs in the combination $\tau = m\theta + kz$, it was shown that the fields could be derived from Eq. (XII 6). In lowest order tokamak ordering where B_z = constant, this is sufficient to solve for B_r and B_θ. (We consider only lowest order tokamak ordering here). It was also shown that ψ actually is a flux, it is simplest to relate it to the vector potential. By making use of the fact that $B = \nabla \times A$, it is not difficult to show that Eqs. (XII 6) follow if

$$\psi = kr A_\theta - m A_z \qquad \text{(XIV 1)}$$

To continue, we will relate ψ to the flux through a helical ribbon at radius r and pitch defined $\tau = kz + m\theta$ = constant. The flux through it is of course just the line integral of $\underline{A}$ around it. A unit vector parallel to the edge of the ribbon is

$$\frac{i_z - \frac{kr}{m} i_\theta}{\left[1 + \left(\frac{kr}{m}\right)^2\right]^{1/2}} \approx i_z - \frac{kr}{m} i_\theta$$

making use of lowest order tokamak ordering. Therefore the magnetic flux through the ribbon is given by $2\pi R \psi$, where R is, as usual, the major radius of the torus. Hence ψ is indeed the helical flux.

We now further specialize to the case of $k = -1/R$, $m = 1$ and examine the form of $\psi(r)$. As shown in Chapter XII, $\psi' = 0$ at the resonant surface where $q = \frac{rB_z}{RB_\theta} = 1$. The second derivative of ψ at the resonant surface is

$$\frac{d^2\psi}{dr^2} = \frac{dB_\theta}{dr} - \frac{B_z}{R} = -B_\theta \frac{dq}{dr} < 0 \qquad \text{(XIV 2)}$$

where we have assumed the normal tokamak profile having $q' > 0$. Thus ψ has a maximum at resonant surface and has the r dependence shown in Fig. (XIV 1a).

Let us now examine how magnetic reconnection could proceed in an $m = 1$ internal disruption. The magnetic flux through a ribbon of width dr is $\frac{d\psi}{dr}\,dr$. Thus the helical fields, on each side of the singular surface, oppose each other. As the fluid inside the singular surface convects toward one side, regions of plasma with opposing helical fluxes are forced together. If the helical flux surfaces maintain their topological structure, as they would in ideal MHD, then Rosenbluth, Dagazian and Rutherford (Phys. Fluids 16, 1894 (1973)) worked out a nonlinear theory for the assymptotic displacement of the plasma. They did this by balancing the driving force against the additional restraining force of the compressed field. They found that the plasma interior is displaced only slightly, for instance if the initial constant ψ surfaces are shown in Fig. (XIV 2a), the final constant ψ surfaces might appear as in Fig. (XIV 2b).

Notice however that in this final state, regions of opposite helical field (along a-b) are forced together. If reconnection is allowed in this region, the large flux compression will not occur and the plasmas sideways displacement can proceed. Let us look into this reconnection more carefully. Since the magnetic field always has zero divergence, two

different regions can reconnect only if they have equal helical flux. Thus, as illustrated in Fig. (XIV 1a), the field at r_1 can connect with the field at r_2. If the layers at r_1 and r_2 have widths dr_1 and dr_2, the fact that the fluxes which reconnect are equal means

$$\left.\frac{d\psi}{dr}\right|_{r_1} dr_1 = -\left.\frac{d\psi}{dr}\right|_{r_2} dr_2 \qquad \text{(XIV 3)}$$

These two flux elements will, at $t = \infty$, come to rest at a position r having width dr. Since the fluid motion is incompressible

$$r\,dr = r_1\,dr_1 + r_2\,dr_2 \qquad \text{(XIV 4)}$$

Also, since the reconnection occurs only at one point, (around a-b), the flux is undisturbed in most of the flux tube so

$$d\psi = d\psi_2 \qquad \text{(XIV 5)}$$

Thus as the field reconnects, the total helical flux in the reconnecting fluid elements is conserved.

It is not difficult to follow this reconnection process. Initially flux tubes 1 and 2 connect as shown in Fig. (XIV 3 a & b) and an island labeled I is formed opposite to the direction of the kink. In this island, the helical field is clockwise, as it is outside of the original q = 1 surface. Therefore the island has q > 1. Later flux elements 3 and 4 reconnect and island II is formed outside of I as shown in Fig. (XIV 3c). The reconnection process completes itself when flux elements 5 and 6 connect to form island III (Fig. (XIV 3d) at the position where $\psi(r) = \psi(o)$ Since all field lines are now clockwise, q is everywhere greater than unity and the plasma has returned to a stable state. Thus the flux near the original q=1 surface has moved to the center and the

flux initially at the center has moved to the outside. The $\psi(r)$ curve then evolves to a monotonically decreasing function of r in which the area between two values of ψ is the same at $t = \infty$ as at $t = 0$. This is illustrated in Fig. (XIV 1b) where the helical flux at $t = \infty$ is shown.

Thus, without invoking any details of a particular $m = n = 1$ instability, Kadomtsev is able to derive the field configuration of a final stable state from an initial unstable state. Once the plasma reaches a stable state, the channeling of the current into the hotter regions will drive the plasma unstable, as discussed in Chapter X. Therefore a relaxation oscillation will ensue.

It is worthwhile to briefly compare Kadomtsev's theory of $m = n = 1$ instability with the quasi-linear theory of Chapter X. The later derived a diffusion equation and ultimately flattened the current profile within the $q = 1$ surface. Then some other mechanism was invoked to spread the current beyond the original $q = 1$ surface to produce a plasma with $q > 1$ everywhere. **Kadomtsev's theory however postulates a coupling between the plasma inside and outside of the $q = 1$ surface so that only his mechanism is needed to produce a plasma with $q > 1$ everywhere.**

We now turn our attention to a very brief survey of numerical simulations of MHD unstable plasmas. There has been a great world wide effort in such simulations recently and many people now feel that this offers the best hope for learning about the nonlinear theory of MHD instabilities. Generally speaking, these simulations are of two types. The first type, pioneered by Rosenbluth and his co-workers at Princeton, assumes helical symmetry,incompressible flow, tokamak ordering and constant density. The full set of three dimensional MHD equations then reduce to two equations for ψ and the z component of the velocity vector

potential in the two dimensional r,τ space. The second approach is to simply solve the full set of MHD equations in three dimensions. Here the plasma is generally assumed to fill either a rectangular solid, or else a torus with rectangular cross section. The first method allows much greater resolution, principally because the helical symmetry reduces the dimensionality from three to two. The second method, of course, has much greater flexibility.

The m = 1 internal kink-tearing mode has been simulated both ways. In each case, care must be taken to allow sufficient resolution in the singular layer. This has necessitated the use of resistivity much larger than that existing in tokamak plasmas.

A two dimensional simulation of the kink tearing mode was performed by Waddell, Rosenbluth, Monticello and White (Nuclear Fusion 16, 528 (1978)). A current density

$$J_z(r) = \frac{J_o}{\left[1 + \left(r/r_o\right)^2\right]^2} \qquad \text{(XIV 6)}$$

is set up at t = 0. J_o is chosen so that q(r = 0) = 0.9 and r_o = 0.6a where a is the radius of the conducting wall. For this current profile, the radius of the q = 1 surface is at r_s = 0.2a and the radius at which the helical flux ψ has the same value as it does at r = 0 is $r_\psi \approx$ 0.3a. Island formation is observed, but the helical flux surfaces become quite complicated very quickly, with multiple island structure developing. What is simpler are the flow patterns, shown at four times in Fig. (XIV 4). This shows that the basic flow pattern of an m = 1 mode persists well into the nonlinear regime. Kadomtsev's theory indicates there should be reconnection out to r_ψ = 0.3a. The perturbed flow and perturbed field

seem to be limited to radii somewhat smaller than this, but accurate resolution is difficult. Also, Waddell et al show the total current as a function of radius, and this is shown in Fig. (XIV 5). Clearly, the simple quasi-linear theory, which predicts current diffusion within the singular surface, is reasonably accurate.

A full three dimensional simulation of this instability was done by Sykes and Wesson (Phys. Rev. Lett, 37, 140, (1976)). By assuming a resistivity with the functional form $\eta \sim T^{-3/2}$, they were able to simulate several cycles of the relaxation oscillation. In Fig. XIV are shown various curves of constant ψ surfaces. Here it can be seen that an island with $q > 1$ grows and ultimately displaces the original flux surfaces having $q < 1$. However different cycles of the relaxation oscillation are not all alike. On other cycles, the original island may return and displace the newly formed island. In this case the original island relaxes to a state having $q > 1$.

It is clear that num erical simulation can be a very powerful technique for the study of the nonlinear behavior of MHD instabilities. However, as these two simulations illustrate, different types of simulations of the same process do not necessarially give exactly the same result. Undoubtedly there will be many more such simulations in the future. In fact, many different instabilities have already been studied by simulations, including tearing modes, internal kinks and free boundary kinks.

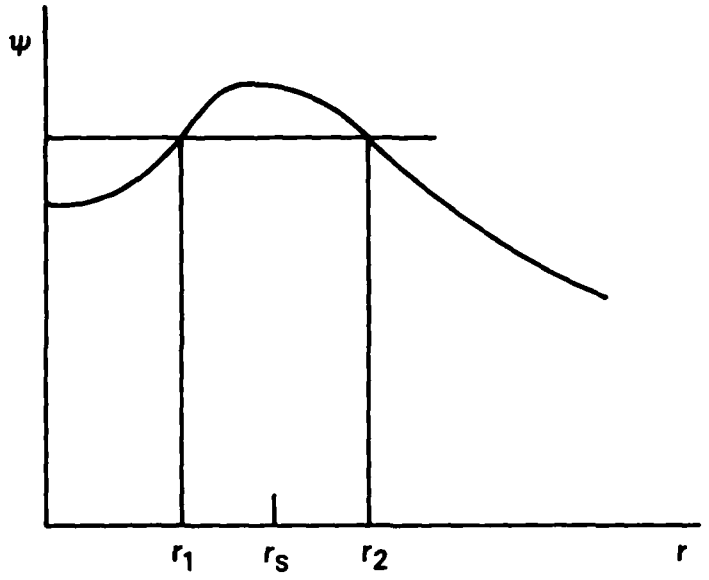

(a)

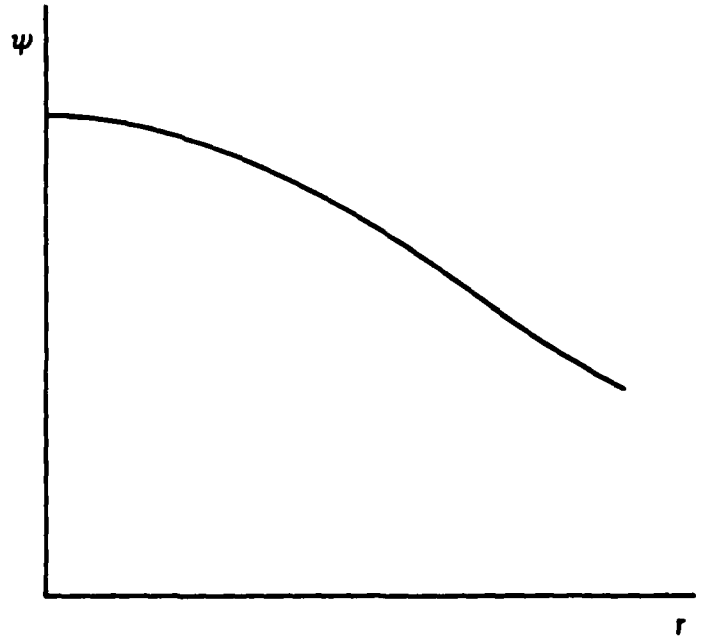

(b)

XIV 1) Initial and final plots of $\psi(r)$ according to Kadomtsev's theory

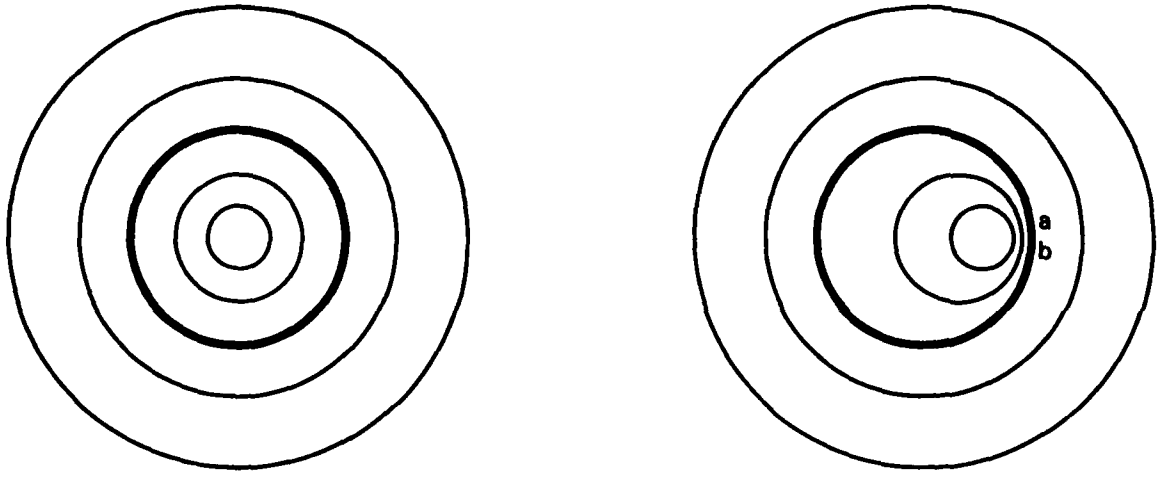

XIV 2) Initial and final plots of flux surfaces in ideal MHD according to Rosenbluth, Dagazian and Rutherford

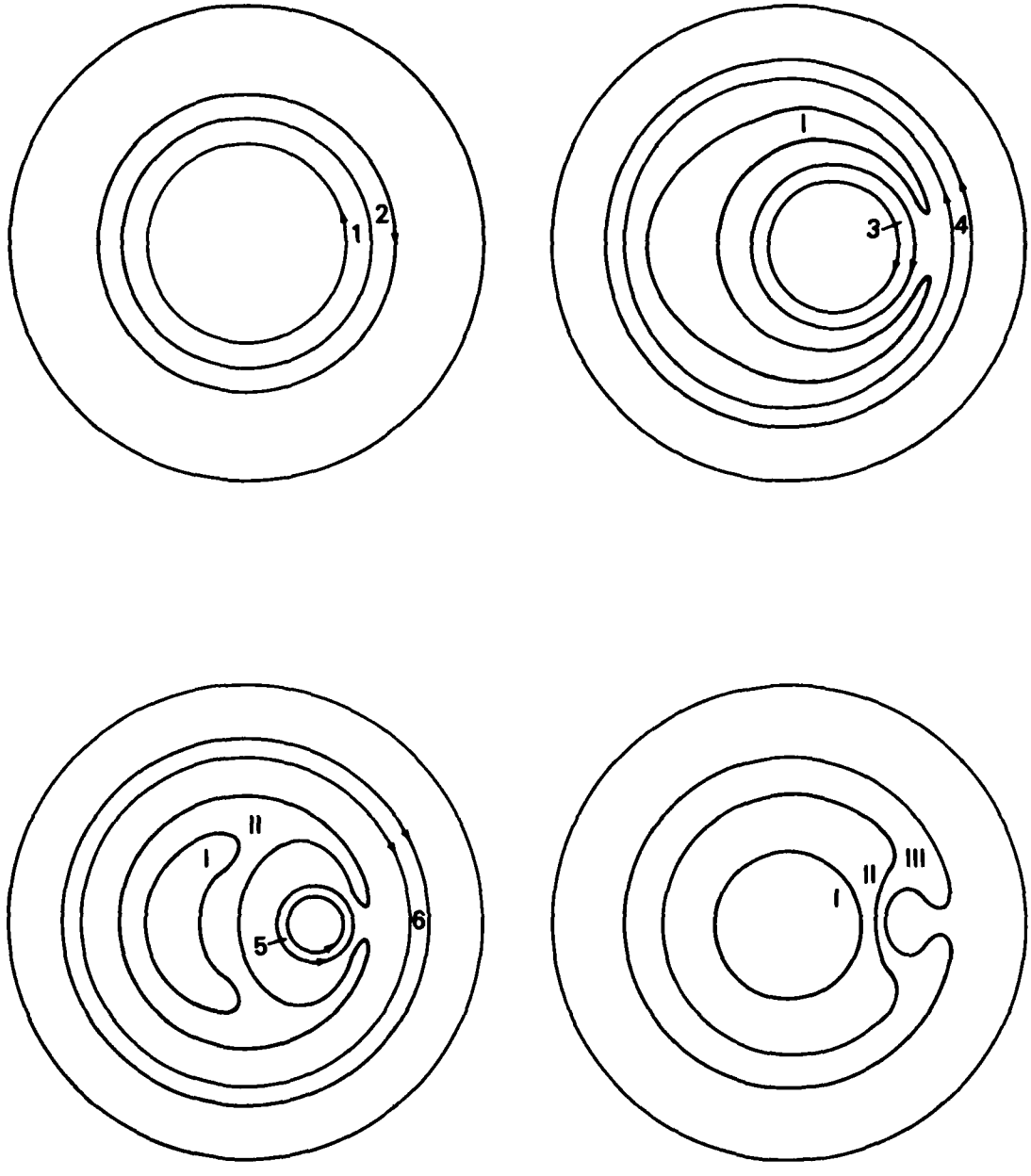

XIV 3) The reconnection process as envisioned by Kadomtsev

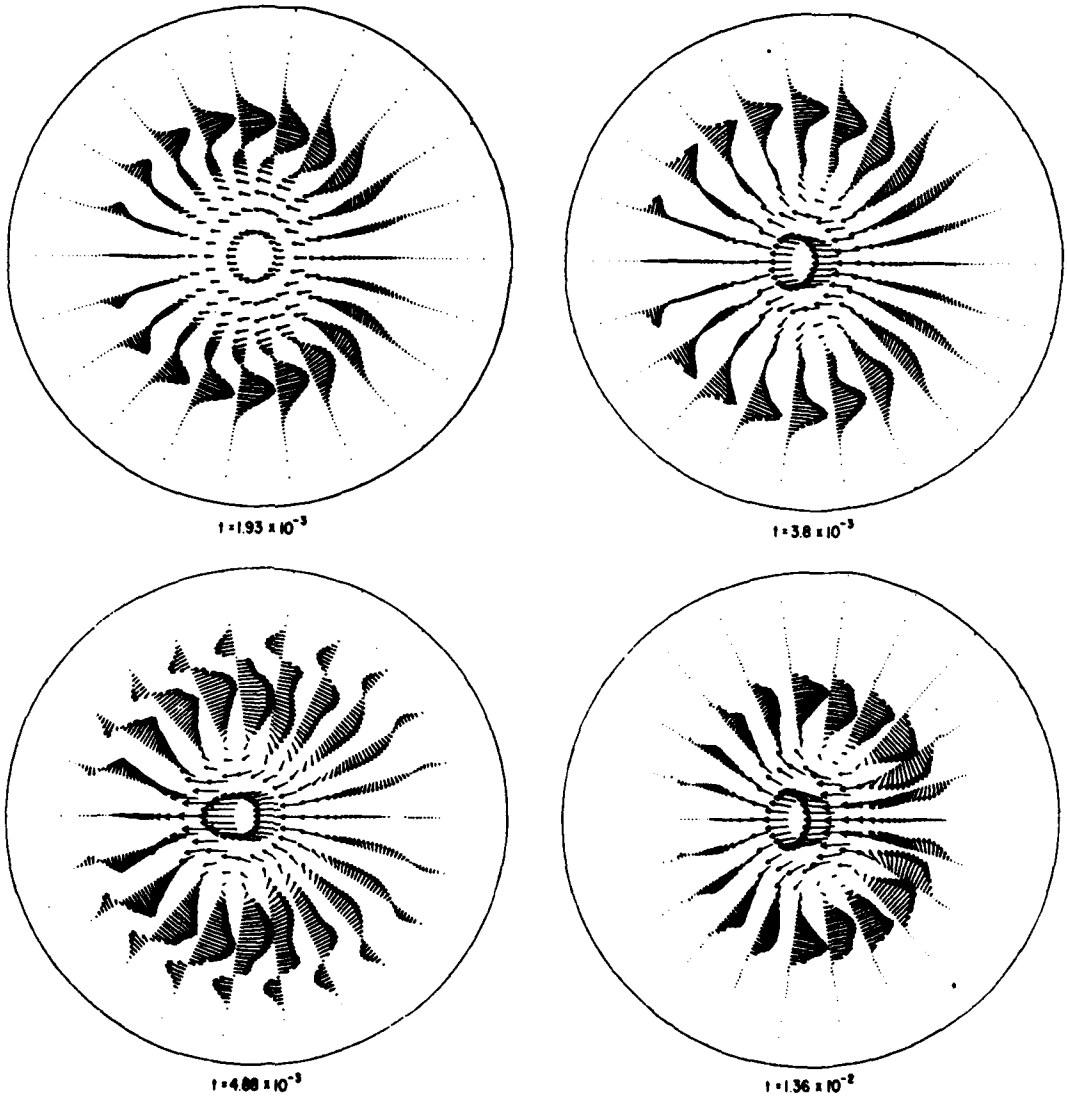

XIV 4) The time evolution of the flow pattern for this instability as computed by Waddell et al

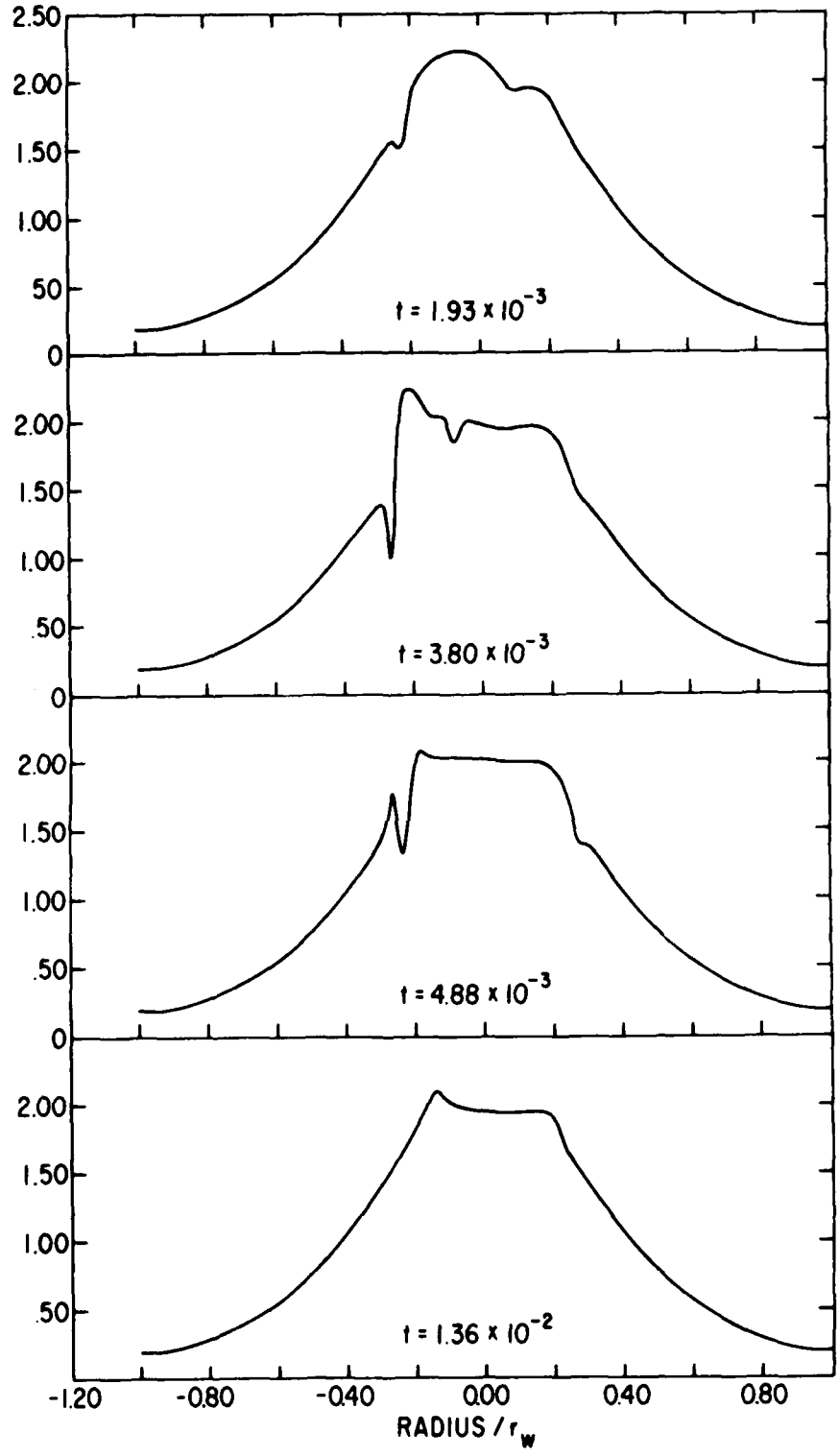

XIV 5) The time evolution of the toroidal current profile as computed by Waddell et al.

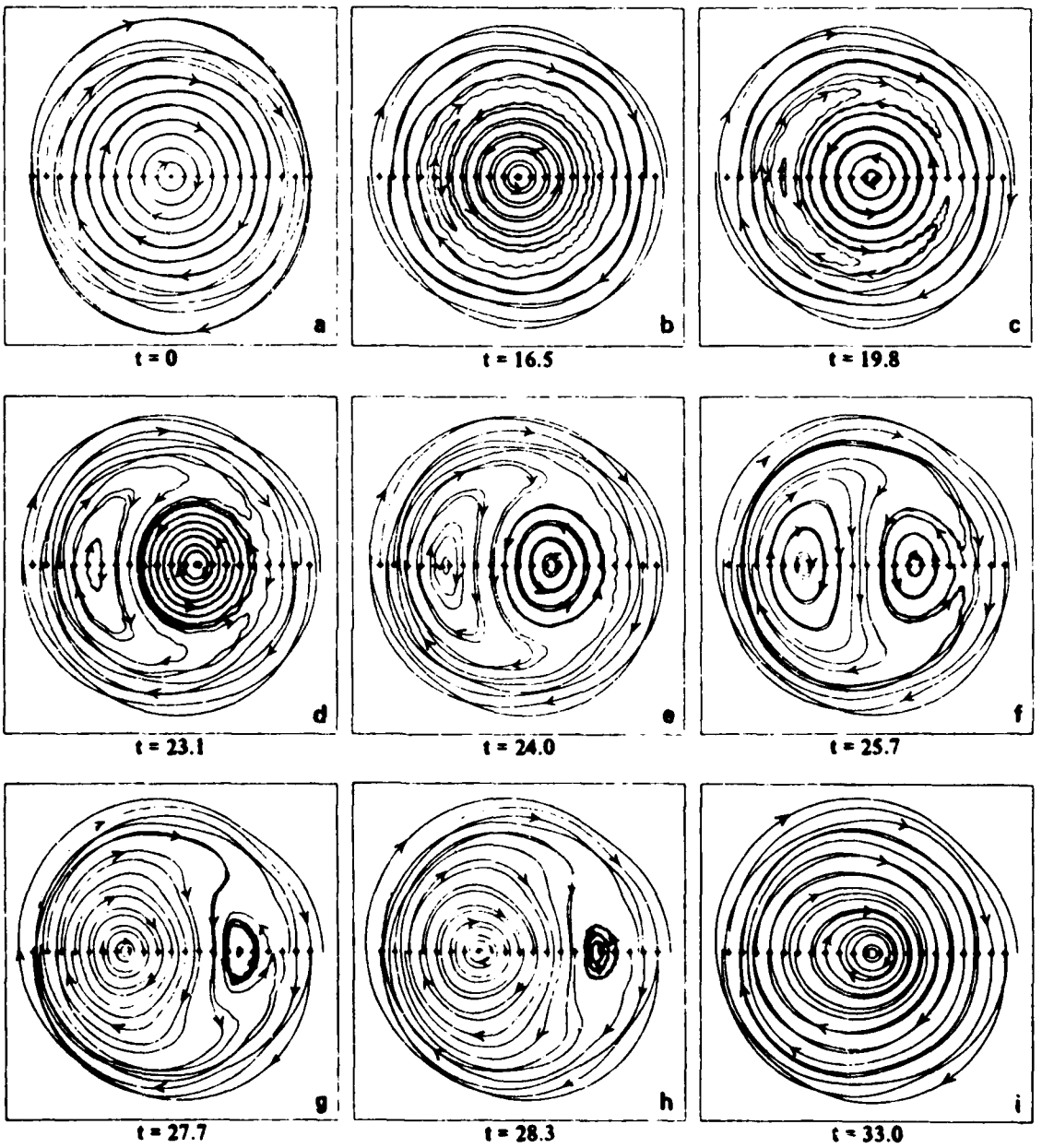

XIV 6) The time evolution of the magnetic surfaces as computed by Sykes and Wesson


DAT
FILM